Ceramide 1-phosphate (C1P) induces macrophage chemoattractant protein-1 release: involvement in C1P-stimulated cell migration.

Lide Arana, Marta Ordoñez, Alberto Ouro, Io-Guané Rivera, Patricia Gangoiti, Miguel Trueba, and Antonio Gomez-Muñoz

Department of Biochemistry and Molecular Biology, Faculty of Science and Technology,

University of the Basque Country (UPV/EHU), 48080 Bilbao (Spain)

Running titled: Stimulation of MCP-1 release by ceramide 1-phosphate

Contact information

Corresponding author:

Prof. Antonio Gómez Muñoz

Department of Biochemistry and Molecular Biology

Faculty of Science and Technology

University of the Basque Country (UPV/EHU)

P.O. Box 644

48080 - Bilbao (Spain)

Tel: 34-94-601 2455 (Direct)

Fax: 34-94- 601 3500

E-mail: antonio.gomez@ehu.es

Keywords

Ceramide 1-phosphate, monocyte chemoattractant protein-1 release, macrophage migration, sphingosine 1-phosphate.

Glossary

C1P, ceramide 1-phosphate

CCR2, C-C chemokine receptor type 2

ERK, extracellularly regulated kinases

FBS, fetal bovine serum

FCS, fetal calf serum

JNK, c-Jun N-terminal kinase

MCP-1, monocyte chemoattractant protein-1

MEK, mitogen activated protein kinase kinase

NF-κB, nuclear factor-kappa B

PBS, phosphate-buffered saline

PI3K, phosphatidylinositol 3-kinase

Ptx, pertussis toxin

S1P, sphingosine 1-phosphate

S1PR, sphingosine 1-phosphate receptor

Abstract

The bioactive sphingolipid ceramide 1-phosphate (C1P) is implicated in inflammatory responses, and was recently shown to promote cell migration. However, the mechanisms involved in these actions are poorly described. Using J774A.1 macrophages we have now discovered a new biological activity of C1P: stimulation of monocyte chemoattractant protein-1 (MCP-1) release. This novel effect of C1P was pertussis toxin (Ptx)-sensitive, suggesting the intervention of Gi protein-coupled receptors. Treatment of the macrophages with C1P caused activation of the phosphatidylinositol 3-kinase (PI3K)/Akt (also known as protein kinase B), mitogen-activated protein kinase kinase (MEK)/extracellularly regulated kinases (ERK), and p38 pathways. Inhibition of these kinases using selective inhibitors or specific siRNA blocked the stimulation of MCP-1 release by C1P. C1P stimulated nuclear factor-kappa B activity, and blockade of this transcription factor also resulted in complete inhibition of MCP-1 release. Also, C1P stimulated MCP-1 release and cell migration in human THP-1 monocytes and 3T3-L1 preadipocytes. A key observation was that sequestration of MCP-1 with a neutralizing antibody, or treatment with MCP-1 siRNA abolished C1P-stimulated cell migration. Also, inhibition of the pathways involved in C1P-stimulated MCP-1 release completely blocked the stimulation of cell migration by C1P. It can be concluded that C1P promotes MCP-1 release in different cell types and that this chemokine is a major mediator of C1P-stimulated cell migration. The PI3K/Akt, MEK/ERK, and p38 pathways are important downstream effectors in this action.

Introduction

Regulation of cell migration is a complex process involving hundreds of molecules. It is necessary for tissue homeostasis, and is crucial for regulation of vital biological processes including embryogenesis, organogenesis, or regeneration [reviewed in (38, 48)]. Also, cell migration is fundamental to inflammatory responses (1, 49), but inadequate migratory signals may induce the migration of the wrong cell type to the wrong place, which may have severe effects in the organism. Some examples include autoimmune syndromes, angiogenesis or the process of metastasis. Although cell migration is a subject of intense investigation, the mechanisms involved in controlling cell movements are incompletely understood. In this connection, growing evidence suggests that some sphingolipids are key metabolites for controlling chemotaxis (52). Our group recently reported that ceramide 1-phosphate (C1P), a sphingolipid metabolite that is present in serum or plasma (25), and which we found to regulate cell growth and survival (15, 17, 18, 20, 22), is a chemoattractant molecule for macrophages (23). This finding is particularly relevant when considering that macrophages play critical roles in chronic and acute inflammation, and that these cells facilitate cancer cell migration (21, 46). In addition, Barth and coworkers (4) recently showed that ceramide kinase, the enzyme responsible for the phosphorylation of ceramide to C1P, regulates NADPH oxidase activity and eicosanoid biosynthesis in neuroblastoma cells, an action that is consistent with our recent finding that C1P increases the production of reactive oxygen species through activation of NADPH oxidase in macrophages (2). Besides these proinflammatory actions, increasing evidence suggests that C1P can aslo function as an antiinflammatory agent under different experimental settings. Specifically, Hankins et al (26) recently reported that C1P reduces lipopolisaccharide (LPS)-mediated nuclear factor-kappa B (NF-κB) activation and cytokine secretion, and Goldsmith et al (16) reported that phosphoceramide analogue-1

(PCERA-1) simultaneously suppresses TNFα and induces the production of antiinflammatory interleukin-10 in activated macrophages.

The most important chemokine that regulates the migration and infiltration of monocytes/macrophages and works as a key factor in initiating the various inflammatory responses is monocyte chemoattractant protein-1 (MCP-1, also known as chemokine (C-C motif) ligand 2)) (11). MCP-1-induced migration of monocytes is mediated through interaction with its receptor CCR2, a Gi protein-coupled receptor (10). There are two subtypes of MCP-1 receptors, CCR2 a and b, with the CCR2b receptor isoform being about five-fold more sensitive to induction of chemotaxis by MCP-1 than CCR2a (50). Furthermore, monocytes and activated NK cells express predominantly the CCR2b isoform (10).

The present study was undertaken to examine whether C1P could stimulate the release of MCP-1 by macrophages and to assess whether this cytokine mediates the chemotactic effect of C1P in macrophages.

Materials and Methods

Materials

N-Hexadecanoyl-D-erythro-sphingosine-1-phosphate (C16:0-Ceramide 1-phosphate) (C1P) was supplied by Matreya. Culture media Dulbecco's Modified Eagle's Medium (DMEM) and RPMI (Roswell Park Memorial Institute) were from Lonza. Fibronectin, JE (MCP-1) from mouse, RS 102895, LY 294002, PD 98059, pertussis toxin and SP 600125 were from Sigma-Aldrich. Fetal bovine serum (FBS) and opti-MEM were from Gibco. Nitrocellulose membranes, protein markers, and BCA assay reagents were purchased from Bio-Rad. MCP-1 neutralizing antibody (cell tested) was purchased from eBioscience. β-Actin, GAPDH, S1PR2 (EDG-5) and S1PR4 (EDG-6) antibodies were from Santa Cruz Biotechnology. S1PR1, S1PR3 and S1PR5 antibodies were supplied by Abcam. Other antibodies were from Cell Signaling. Mouse CCL2 (MCP-1) ELISA Ready-SET-Go! was supplied by eBioscience. Oligofectamine^{TM} Reagent was from Molecular Probes (Invitrogen). SC-514 and 10-DEBC were from Tocris. Akt1 siRNA, Mapk1 (Erk2) siRNA, Pik3r1 (PI3K) siRNA, Mapk8 (JNK1) siRNA, Mapk9 (JNK2) siRNA, Mapk10 (JNK3) siRNA, Mapk14 (p38α) siRNA, S1PR1 (s1pr1) siRNA, S1PR3 (s1pr3) siRNA and S1PR4 (s1pr4) siRNA were from Applied Biosystems (Ambion) and CKR-2 siRNA, negative siRNA, S1PR2 (EDG-5) siRNA, S1PR5 (EDG-8) siRNA and MCP-1 siRNA were supplied by Santa Cruz Biotechnology. All of the other chemicals and reagents were of the highest grade available.

Cell culture

The J774A.1, THP-1 and 3T3-L1 cell lines used in this work were purchased from ATCC (Manassas, VA, USA), and were cultured following the manufacturer's indications. J774A.1 macrophages were grown in DMEM supplemented with 10% heat-inactivated

FBS, 50 mg/l of gentamicine, and 200 µM L-glutamine. Cells were incubated at constant temperature (37 ºC) in a humidified atmosphere containing 5% CO_2. The THP-1 cells were grown in RPMI supplemented with 10% heat-inactivated FBS, 25 mg/l of gentamicine, and 200 µM L-glutamine. The cells were incubated at constant temperature (37 ºC) in a humidified atmosphere containing 5% CO_2. The 3T3-L1 cell line was grown in DMEM supplemented with 10% heat-inactivated FCS, 4.5 g/l of D-glucose, 50 mg/l of gentamicine, and 200 µM L-glutamine. Cells were incubated at constant temperature (37 ºC) in a humidified atmosphere containing 5% CO_2.

Bone marrow-derived macrophages (BMDM) were isolated from femurs of 6-8-week old female CD-1 mice as described (24). Cells were plated for 24 h in RPMI 1640 medium containing 10% fetal bovine serum (FBS) and 10% L-cell conditioned medium as the source of macrophage-colony stimulating factor (M-CSF) (27). The non-adherent cells were removed and cultured for 4-6 days in the same medium until about 80% confluence was reached.

Delivery of C1P to cells in culture

An aqueous dispersion (in the form of liposomes) of C1P was added to cultured macrophages as previously described (15, 19, 20). Specifically, stock solutions were prepared by sonicating C1P (5 mg) in sterile nanopure water (3 ml) on ice using a probe sonicator until a clear dispersion was obtained. The final concentration of C1P in the stock solution was approximately 2.62 mM. This procedure is considered preferable to dispersions prepared by adding C1P in organic solvents because droplet formation is minimized and exposure of cells to alcohols or dodecane is avoided.

Measurement of MCP-1 concentration

J774A.1 macrophages were seeded in 24-well plates (2×10^4 cells/well) and incubated in 0.525 ml of DMEM containing 10% FBS, overnight. The next day, the cells were washed

twice with PBS, and the medium was replaced by fresh DMEM containing 1% FBS. Macrophages were incubated for two additional hours and agonists were then added as required. After incubation, the cell media were collected into microcentrifuge tubes and cells were scrapped for counting. The 3T3-L1 preadipocytes were seeded in 24-well plates (10^4 cells/well) and incubated in DMEM containing 10% FCS, overnight. The next day, the cells were washed twice with PBS, and the medium was replaced by fresh DMEM in the absence of FCS. Cells were incubated for two additional hours and agonists were then added as required. Then, the media were collected and cells were trypsinized for counting. THP-1 cells were seeded in 24-well plates (10^5 cells/well) and incubated in 0.5 ml of RPMI. After two hours, agonists were added as required. Then, cell media along with monocytes were collected into microcentrifuge tubes and cells were counted. The harvested media were centrifuged at 10,000 ×g for 5 min at 4 ℃ and supernatants were diluted for determination of MCP-1 concentration. The amount of MCP-1 in the medium was determined using a "Mouse CCL2 (MCP-1) ELISA Ready-SET-Go!" kit according to the manufacturer's instructions. Sample concentration values (pg/ml) obtained by the calibration curve were normalized by the number of cells counted in each well or by the amount of protein in each well.

Determination of cell migration.

Cell migration was measured using a Boyden chamber-based cell migration assay, as described (23). Twenty four-well chemotaxis chambers (Transwell, Corning Costar) precoated with 30 µg of fibronectin were used for the experiments. For J774A.1,3T3-L1 and BMDM cell migration studies 8 µm pore size was used, and for THP-1 cells the pore size was 5 µm. Cell suspensions (100 µl, 5 x 10^4 cells for J774A.1; 100 µl, 5 x 10^4 cells for 3T3-L1; 1.5 10^5 cells for BMDM and 100 µl, 10^5 cells for THP-1) were then added to the upper wells of 24-well chemotaxis chambers. Agonists were added to the lower wells

diluted in 300 µl medium supplemented with 0.2% fatty acid-free bovine serum albumin (BSA) and 0.2% FBS treated with activated carbon. When used, inhibitors were added to the upper and lower wells and preincubated for 1 h prior to agonist addition. Non-migrated cells were removed with a cotton swab, and the filters were fixed with formaldehyde (5% in PBS) and stained with hematoxilyn-eosin. Cell migration was assessed by counting the number of migrated cells in a Nikon Eclipse 90i microscope equipped with NIS-Elements 3.0 software. Cells were counted in six randomly selected microscopy fields per well at 20× magnification.

Treatment of cells with small interfering RNA

siRNA transfection protocols were performed following the manufacturer's instructions. Cells were seeded in 60 mm diameter plates (2 x 10^5 cells/well) in DMEM containing 10% FBS. The medium was replaced by 1.6 ml opti-MEM and cells were then incubated for 24 h. Twenty pmol per ml of siRNA in 0.4 ml of opti-MEM were added into each well. Cells were then incubated for 4-5 h and 2 ml of opti-MEM containing 20% FBS were then added to the wells, without removing the transfection mixture. The cells were incubated further for 24 h and the medium was then replaced by fresh DMEM containing 10% FBS. Cells were scrapped and counted, and then used for experiments.

Western blotting

Cells (0.25×10^6 cells/plate) were seeded in 60 mm diameter plates in DMEM containing 10% FBS and incubated overnight. The next day, the cells were washed and medium was replaced by DMEM containing 1% FBS. After 2 h agonists were added and cells were further incubated for the indicated periods of time. Macrophages were harvested and lysed in ice-cold homogenization buffer as described (24). About 20–40 µg of protein from each sample was loaded and separated by sodium dodecyl sulfate polyacrylamide gel

electrophoresis (SDS–PAGE), using 12% separating gels. Proteins were transferred onto nitrocellulose paper and blocked for 1 h with 5% skim milk in Tris-buffered saline (TBS) containing 0.01% NaN_3 and 0.1% Tween 20, and then incubated overnight with the primary antibody in TBS/0.1% Tween 20 at 4 ℃. After three washes with TBS/0.1% Tween 20, membranes were incubated with horseradish peroxidase- conjugated secondary antibody at 1:4000 dilution for 1 h. Thereafter the proteins were visualized by enhanced chemiluminescence.

Statistical analyses

Results are expressed as mean ± SEM of three to six independent experiments performed in triplicate, unless indicated otherwise. Confirmation for siRNA inhibition of each particular siRNA-targeted protein are expressed as the mean ± range of two independent experiments. Statistical analyses were performed using the two-tailed, paired Student's t-test, where $p < 0.05$ was considered to be significant (GraphPad Prism software, San Diego, CA).

Results

Ceramide 1-phosphate stimulates MCP-1 release in J774A.1 macrophages.

Leukocyte chemotaxis toward sites of inflammation or tumorigenesis is primarily mediated by chemokine signaling (37), and we have demonstrated that C1P stimulates macrophage migration (23). A major chemokine that regulates the migration and infiltration of macrophages is MCP-1. Fig. 1 shows that C1P significantly stimulated the release of MCP-1 by J774A.1 macrophages in a concentration (panel A) and time dependent manner (panel B). Optimal MCP-1 release was attained at 20 µM C1P after 24 h of incubation. A similar fold increase of MCP-1 release was still observed after 48 h of incubation with 20 µM C1P (Fig. 1B). Although this optimal concentration of C1P is relatively high compared to plasma levels (around 0.5 µM) (25), it was shown that C1P concentrations vary according to the nutritional state of the organism and can be secreted by macrophages (5, 25) or by leaky damaged cells (29), so that local concentrations of C1P in vivo can be much higher than 0.5 µM. In addition, it was reported that ATP at physiological concentrations (0.1 mM) can elevate intracellular C1P up to about 4-5 nmoles per million cells (32). So, if this amount of C1P were released into the extracellular milieu, local concentrations of around 5-10 µM, or even higher, would be easily achievable, right after secretion. Also, in this work, C1P was added to the cells in the form of liposomes (sonicated in water) and so, the actual concentration of C1P that a cell "sees" is much lower than what is added to the culture medium. Therefore, the effective concentrations of C1P used in these experiments can be considered to be within or very close to physiological levels.

C1P-stimulated MCP-1 release is mediated by the PI3K/Akt (PKB), MEK/ERK1-2 and p38 pathways.

We showed previously that C1P was able to stimulate PI3K/Akt (PKB) and MEK/ERK1-2, and that these pathways were involved in the mitogenic (15) and chemotactic (23) effects of C1P. Therefore, we tested to see whether these pathways were implicated in the release of MCP-1 by C1P. First, selective inhibitors of PI3K and Akt, as well as specific siRNA to silence the expression of the genes encoding these kinases were used. Fig. 2 (panels A and B) shows that the PI3K inhibitor LY 294002 (1 µM) or 10-DEBC (1µM), an inhibitor of Akt, completely inhibited C1P-stimulated MCP-1 release. Likewise, pre-incubation of these cells with specific siRNAs to silence PI3K or Akt1 completely blocked the stimulation of MCP-1 release by C1P (Fig. 2C, D). Western-blotting demonstrated potent knockdown of PI3K (Fig. 2E, F), or Akt1 (Fig. 2G, H) with 20 pmol/ml PI3K-targeted or Akt-targeted siRNA, respectively. To evaluate the possible involvement of MAP kinases in this process the MEK inhibitor PD 98059, and specific siRNA against extracellularly regulated kinases (ERK) were used. Both of these agents completely blocked C1P-stimulated MCP-1 release (Fig 3A, B). Western-blotting demonstrated potent knockdown of ERK (Fig. 3C, D) with 20 pmol/ml ERK-targeted siRNA. In addition, the p38 inhibitor SB 202190, and siRNA against p38α significantly decreased the stimulation of MCP-1 release by C1P (Fig. 4A, B). Western-blotting demonstrated potent knockdown of p38α (Fig. 4C, D) with 20 pmol/ml p38α-targeted siRNA. However, specific siRNAs against the three different JNK isoforms (JNK 1-3), although potently inhibited, did not significantly alter C1P-stimulated MCP-1 release suggesting that this kinase is not involved in this process (Fig 5). The effect of C1P on stimulation of ERK1-2, p38α, and Akt phosphorylation is shown on Fig. 6.

A well-known downstream target of Akt and ERK1-2 is NF-κB, a transcription factor that plays an essential role in the induction of inflammatory mediators. The activation of NF-κB by C1P in the J774A.1 macrophages was evaluated by determining

its phosphorylation state after treatment with C1P. Fig. 7 (A, B) shows that C1P increases phosphorylation of NF-κB in a time-dependent manner, which is consistent with NF-κB activation. The implication of NF-κB in C1P-stimulated MCP-1 release was evaluated using SC-514, a selective inhibitor of this transcription factor. This inhibitor completely blocked the release of MCP-1 that was stimulated by C1P (Fig. 7C).

MCP-1 is essential for stimulation of cell migration by C1P.

We reported recently that C1P promotes RAW264.7 leukemia monocytic cell migration, and that the PI3K/Akt and MEK/ERK pathways were involved in this process (23). These observations together with the results shown above led us to hypothesize that MCP-1 might be the key mediator of C1P-stimulated macrophage migration. The ability of MCP-1 to stimulate macrophage migration was studied by incubating the cells with increasing concentrations of MCP-1. Fig. 8 shows that MCP-1 stimulates macrophage migration in a concentration (panel A) and time (panel B) dependent manner. Of interest, MCP-1 was as potent as C1P at stimulating cell migration (Fig. 8A, C). To evaluate whether the release of MCP-1 was required for the stimulation of macrophage migration by C1P, two different experimental approaches were used. First, the cells were preincubated with a specific monoclonal antibody against MCP-1 prior to stimulation with C1P, and second, the macrophages were pretreated with specific MCP-1 siRNA. Both of these treatments completely blocked C1P-stimulated macrophage migration (Fig. 9), thereby demonstrating that MCP-1 release is absolutely required in this process. Western-blotting demonstrated potent knockdown of MCP-1 (Fig. 9C, D) with 20 pmol/ml MCP-1-targeted siRNA. Two key observations that further supported this hypothesis were that RS 102895, a selective inhibitor of the MCP-1 receptor CCR2b (Fig. 10A), and siRNA against this receptor (Fig. 10B), completely blocked both MCP-1- and C1P-stimulated

macrophage migration (Fig. 10). Western-blotting demonstrated potent knockdown of CCR2b (Fig. 10C, D) with 20 pmol/ml CCR2b-targeted siRNA.

C1P-stimulated migration of J774A.1 macrophages involves activation of the PI3K/Akt (PKB), MEK/ERK1-2 and p38 pathways.

The observation that MCP-1 release is essential for the stimulation of macrophage migration by C1P, suggested that the pathways involved in C1P-stimulated MCP-1 release might also be implicated in cell migration. This was examined using selective inhibitors of these pathways (PD 98059 to inhibit MEK, 10-DEBC to inhibit Akt, and SB 202190 to inhibit p38, as well as specific siRNAs to silence the genes encoding these kinases. All of these inhibitory agents abrogated the induction of macrophage migration by C1P (Fig. 11A, B), suggesting that these pathways are crucial in this process. We previously reported that NF-κB is a downstream target of Akt and ERK, and that C1P stimulated the DNA binding activity of this transcription factor in macrophages (15). In agreement with the latter work, Fig. 11B shows that inhibition of NF-κB blocks C1P-stimulated macrophage migration.

In addition, we show in this work that C1P-stimulated MCP-1 release and macrophage migration are inhibited by pertussis toxin (Ptx) (Fig. 12), which is consistent with our previous studies suggesting the involvement of a Gi protein-coupled receptor in the stimulation of RAW264.7 monocytic leukemia cell migration by C1P (23).

The stimulation of MCP-1 release and cell migration by C1P are independent of interaction with sphingosine 1-phosphate receptors.

Sphingosine 1-phosphate (S1P) is a bioactive sphingolipid that is closely related to C1P. In fact, like the C1P receptor, S1P receptors are also coupled to Gi proteins and sensitive to inhibition by Ptx (13, 52). There are five S1P receptors, which are named S1PR1-5.

Therefore, it could be speculated that C1P might be able to interact with any of these receptors to stimulate MCP-1 release and cell migration. To test this possibility, we treated the macrophages with specific siRNAs to silence the genes encoding for each S1PR. Figure 13 shows that pretreating cells with specific S1PR siRNAs did not significantly affect C1P-stimulated MCP-1 release (panel A) or cell migration (panel B), thereby demonstrating that these effects of C1P are independent of interaction with S1P receptors. Western-blotting demonstrated potent knockdown of S1PR1 (panels C, D), S1PR2 (panels E, F), S1PR3 (panels G, H), S1PR4 (panels I, J), and S1PR5 (panels K,L) with 20 pmol/ml of each S1PR-targeted siRNA.

C1P stimulates MCP-1 release and cell migration in human THP-1 monocytes and 3T3-L1 preadipocytes.

In addition to stimulating MCP-1 release and cell migration in murine macrophages, we found that C1P also exerted these actions on other cell types including human THP-1 monocytes, and 3T3-L1 preadipocytes. Figure 14 shows that C1P promoted MCP-1 release (panel A) and cell migration (panel B) in THP-1 cells, and that migration was inhibited when the cells were incubated in the presence of a specific antibody to MCP-1 (Fig. 14C), in analogy to the results obtained in J774A.1 macrophages (Figs. 1, 8, and 9). Likewise, C1P was able to stimulate MCP-1 release (Fig. 15A) and cell migration (Fig. 15B) in 3T3-L1 preadipocytes, and these effects were also abolished in the presence of a specific antibody to MCP-1 (Fig. 15C).

Discussion

We reported recently that C1P stimulates cell migration in RAW264.7 cells (23). Although this finding has increased our knowledge on how chemotaxis can be regulated in cells, the mechanisms or signaling pathways involved in this process are only

beginning to be elucidated. In the present study we present strong evidence for a novel action of C1P: stimulation of MCP-1 secretion. This chemokine plays an important role in the recruitment of mononuclear cells into sites of inflammation and has been associated to tumor metastasis (7, 41, 57). This proinflammatory action of C1P is consistent with previous work by Chalfant and co-workers, who found that this phosphosphingolipid potently stimulates calcium-dependent cytosolic phospholipase A_2 (cPLA$_2$) activity and the subsequent generation of arachidonic acid and prostaglandins leading to inflammation (43-45). Although C1P can increase prostaglandin synthesis, it is unlikely that they participate in the stimulation of MCP-1 production and stimulation of cell migration by C1P as prostaglandins were reported to inhibit MCP-1 production (53). Supplementary Fig 1 confirms the latter observation (panel A), and shows that C1P-stimulated macrophage migration can be inhibited by prostaglandin E2 (panel B). MCP-1 has also been associated with stimulation of cell proliferation in both healthy and malignant cells (7, 55), and although it did not affect the growth of bladder cancer cells, it mediated migration and invasion of those cells (9), and facilitated metastasis to bone, lung and prostate (6, 36, 47, 57).

There are several pathways involved in the regulation of secretion of chemokines, and we showed previously that C1P could activate some of these pathways (3, 14). In particular, we found that C1P was able to stimulate PI3K/Akt (PKB) and MEK/ERK1-2, and that these pathways were involved in the mitogenic (15) and chemotactic (23) effects of C1P. In the present study, we demonstrate that C1P-stimulated MCP-1 release is mediated by these pathways. In addition, we found that C1P promoted phosphorylation of the MAP kinase p38, and that blockade of this enzyme activity using siRNA or chemical inhibition completely abrogated C1P-stimulated MCP-1 release. Moreover, C1P-stimulated MCP-1 release was completely abolished by Ptx, an action that is

compatible with the existence of a specific Gi protein-coupled receptor for C1P (23). The implication of Akt, ERK1-2 and p38 in this C1P action is consistent with previous work by other groups showing that MCP-1 upregulated these kinases in different cell types including rat aortic smooth muscle cells (55), proximal tubular cells (51), 3T3-L1 preadipocytes (56), vascular smooth muscle cells (12), or monocytes (33). Nonetheless, although MCP-1 release has been associated to activation of p38 in many instances [(8, 33, 56), and our own work] other studies indicated that this kinase is not involved in this process (31, 35), and therefore the role of p38 in stimulation of MCP-1 secretion remains controversial.

Of note, two related phosphosphingolipid mediators, sphingosine phosphorylcholine (SPC) and sphingosine 1-phosphate (S1P), also induced secretion of proinflammatory MCP-1 in human umbilical vein endothelial cells (34) and vascular smooth muscle cells (54), and human mast cells (42), respectively. Like for C1P, the stimulating effect of SPC on MCP-1 secretion was also dependent upon activation of a specific, although still not well defined, receptor (40). However, contrary to C1P, the stimulation of MCP-1 release by S1P was not dependent upon receptor activation (42). In addition, we demonstrate here that C1P-stimulated MCP-1 release and cell migration are independent of interaction of C1P with S1P receptors.

A key observation in this work was that incubation of the macrophages with an MCP-1 neutralizing antibody, or with MCP-1 siRNA, or the MCP-1 receptor antagonist RS 102895 or CCR2b-targeted siRNA, abrogated C1P-stimulated cell migration, thereby demonstrating that MCP-1 is the principal mediator of C1P-stimulated macrophage migration. These findings are consistent with recent work by Mitsutake and coworkers who have recently demonstrated that MCP-1-induced cell migration was significantly reduced in BMDM from mice lacking ceramide kinase, the enzyme responsible for C1P

generation (39). We also observed that C1P was able to stimulate migration of BMDM, but this effect was only marginal compared to the extent of activation seen in J774A.1 macrophages (supplementary figure 2), in agreement with Mitsutake and co-workers (39).

Although the molecular identity of the target receptor whose activation by C1P leads to MCP-1 release and subsequent migration of the macrophages is not yet clear, we show here that a Ptx-sensitive G protein-coupled receptor is likely to be involved in mediating these effects of C1P. In fact, Ptx blocked C1P-stimulated macrophage migration, which is consistent with the inhibition of C1P-stimulated MCP-1 release by this toxin, and with our previous work on RAW264.7 cells (23). These observations suggest that MCP-1 release depends upon the interaction of C1P with its putative receptor to trigger macrophage migration.

In terms of the signaling events downstream of C1P stimulation in macrophages, our previous work showed that PI3K/Akt, MEK/ERK1-2, and JNK are involved in the mitogenic or antiapoptotic effects of C1P, and these pathways are also known to act downstream of the C1P receptor (23). In the present work we found that PI3K/Akt MEK/ERK and their downstream target NF-κB are involved in the stimulation of cell migration by C1P. However, inhibition of JNK did not alter macrophage migration. Of interest, and contrary to PI3K/Akt and MEK/ERK, JNK was also not involved in upregulation of MCP-1 expression in endometrial stroma cells (35).

Finally, it should be emphasized that the effects of C1P on MCP-1 release and cell migration are not restricted to murine macrophages as C1P also promoted these actions in human THP-1 monocytes and 3T3-L1 preadipocytes. Moreover, recent work by Ratajczak's group demonstrates that C1P also stimulates migration of hematopoietic stem progenitor cells (30), multipotent stromal cells and endothelial progenitor cells (29), as

well as migration of bone-marrow derived stem cells in patients suffering from acute myocardial infarction (28).

In conclusion, we demonstrate here that C1P promotes MCP-1 release and cell migration in macrophages. This stimulatory effect of C1P is accomplished through activation of the PI3K/Akt, MEK/ERK1-2 and p38 pathways, but not JNK, via Ptx-sensitive G proteins, leading to NF-κB activation. C1P also stimulated MCP-1 release and migration in human THP-1 monocytes and 3T3-L1 preadipocytes. Because MCP-1 is proinflammatory and may be involved in tumorigenesis and tumor metastasis, C1P and its putative plasma membrane receptor may have potential as therapeutic targets to combat inflammation and cancer.

Acknowledgements

Conflict of interest

The authors declare that there is no conflict of interest associated with this manuscript.

Author contributions

Lide Arana, Marta Ordoñez, Alberto Ouro, Io-Guané Rivera, Patricia Gangoiti, and Miguel Trueba performed research and analysed data. Antonio Gomez-Muñoz supervised the research. Lide Arana and Antonio Gomez-Muñoz designed the experiments and wrote the paper.

References

1.   **Aman A, and Piotrowski T**. Cell migration during morphogenesis. *Dev Biol* 341: 20-33, 2009.

2.   **Arana L, Gangoiti P, Ouro A, Rivera IG, Ordonez M, Trueba M, Lankalapalli RS, Bittman R, and Gomez-Munoz A**. Generation of reactive oxygen species (ROS) is a key factor for stimulation of macrophage proliferation by ceramide 1-phosphate. *Exp Cell Res* 318: 350-360, 2012.

3.   **Arana L, Gangoiti P, Ouro A, Trueba M, and Gomez-Munoz A**. Ceramide and ceramide 1-phosphate in health and disease. *Lipids Health Dis* 9: 15, 2010.

4.   **Barth BM, Gustafson SJ, Hankins JL, Kaiser JM, Haakenson JK, Kester M, and Kuhn TB**. Ceramide kinase regulates TNFalpha-stimulated NADPH oxidase activity and eicosanoid biosynthesis in neuroblastoma cells. *Cell Signal* 24: 1126-1133, 2012.

5.   **Boath A, Graf C, Lidome E, Ullrich T, Nussbaumer P, and Bornancin F**. Regulation and traffic of ceramide 1-phosphate produced by ceramide kinase: comparative analysis to glucosylceramide and sphingomyelin. *J Biol Chem* 283: 8517-8526, 2008.

6.   **Craig MJ, and Loberg RD**. CCL2 (Monocyte Chemoattractant Protein-1) in cancer bone metastases. *Cancer Metastasis Rev* 25: 611-619, 2006.

7.   **Chehl N, Gong Q, Chipitsyna G, Aziz T, Yeo CJ, and Arafat HA**. Angiotensin II regulates the expression of monocyte chemoattractant protein-1 in pancreatic cancer cells. *J Gastrointest Surg* 13: 2189-2200, 2009.

8.   **Chen YC, Chen CH, Ko WS, Cheng CY, Sue YM, and Chen TH**. Dipyridamole inhibits lipopolysaccharide-induced cyclooxygenase-2 and monocyte chemoattractant protein-1 via heme oxygenase-1-mediated reactive oxygen species reduction in rat mesangial cells. *Eur J Pharmacol* 650: 445-450, 2011.

9.   **Chiu HY, Sun KH, Chen SY, Wang HH, Lee MY, Tsou YC, Jwo SC, Sun GH, and Tang SJ**. Autocrine CCL2 promotes cell migration and invasion via PKC activation and tyrosine phosphorylation of paxillin in bladder cancer cells. *Cytokine* 59: 423-432, 2012.

10.   **Deshmane SL, Kremlev S, Amini S, and Sawaya BE**. Monocyte chemoattractant protein-1 (MCP-1): an overview. *J Interferon Cytokine Res* 29: 313-326, 2009.

11.   **Felton LM, Cunningham C, Rankine EL, Waters S, Boche D, and Perry VH**. MCP-1 and murine prion disease: separation of early behavioural dysfunction from overt clinical disease. *Neurobiol Dis* 20: 283-295, 2005.

12.   **Fougerat A, Smirnova N, Gayral S, Malet N, Hirsch E, Wymann M, Perret B, Martinez L, Douillon M, and Laffargue M**. Key role of PI3Kgamma in monocyte chemotactic protein-1-mediated amplification of PDGF-induced aortic smooth muscle cell migration. *Br J Pharmacol* 166: 1643-1653, 2012.

13.   **Fyrst H, and Saba JD**. An update on sphingosine-1-phosphate and other sphingolipid mediators. *Nat Chem Biol* 6: 489-497, 2012.

14.   **Gangoiti P, Camacho L, Arana L, Ouro A, Granado MH, Brizuela L, Casas J, Fabrias G, Abad JL, Delgado A, and Gomez-Munoz A**. Control of metabolism and signaling of simple bioactive sphingolipids: Implications in disease. *Prog Lipid Res* 49: 316-334, 2010.

15.   **Gangoiti P, Granado MH, Wang SW, Kong JY, Steinbrecher UP, and Gomez-Munoz A**. Ceramide 1-phosphate stimulates macrophage proliferation through activation of the PI3-kinase/PKB, JNK and ERK1/2 pathways. *Cell Signal* 20: 726-736, 2008.

16.   **Goldsmith M, Avni D, Levy-Rimler G, Mashiach R, Ernst O, Levi M, Webb B, Meijler MM, Gray NS, Rosen H, and Zor T**. A ceramide-1-phosphate analogue, PCERA-1,

simultaneously suppresses tumour necrosis factor-alpha and induces interleukin-10 production in activated macrophages. *Immunology* 127: 103-115, 2009.

17.	**Gomez-Munoz A, Duffy PA, Martin A, O'Brien L, Byun HS, Bittman R, and Brindley DN**. Short-chain ceramide-1-phosphates are novel stimulators of DNA synthesis and cell division: antagonism by cell-permeable ceramides. *Mol Pharmacol* 47: 833-839, 1995.

18.	**Gomez-Munoz A, Frago LM, Alvarez L, and Varela-Nieto I**. Stimulation of DNA synthesis by natural ceramide 1-phosphate. *Biochem J* 325 (Pt 2): 435-440, 1997.

19.	**Gomez-Munoz A, Kong JY, Parhar K, Wang SW, Gangoiti P, Gonzalez M, Eivemark S, Salh B, Duronio V, and Steinbrecher UP**. Ceramide-1-phosphate promotes cell survival through activation of the phosphatidylinositol 3-kinase/protein kinase B pathway. *FEBS Lett* 579: 3744-3750, 2005.

20.	**Gomez-Munoz A, Kong JY, Salh B, and Steinbrecher UP**. Ceramide-1-phosphate blocks apoptosis through inhibition of acid sphingomyelinase in macrophages. *J Lipid Res* 45: 99-105, 2004.

21.	**Goswami S, Sahai E, Wyckoff JB, Cammer M, Cox D, Pixley FJ, Stanley ER, Segall JE, and Condeelis JS**. Macrophages promote the invasion of breast carcinoma cells via a colony-stimulating factor-1/epidermal growth factor paracrine loop. *Cancer Res* 65: 5278-5283, 2005.

22.	**Granado MH, Gangoiti P, Ouro A, Arana L, and Gomez-Munoz A**. Ceramide 1-phosphate inhibits serine palmitoyltransferase and blocks apoptosis in alveolar macrophages. *Biochim Biophys Acta* 1791: 263-272, 2009.

23.	**Granado MH, Gangoiti P, Ouro A, Arana L, Gonzalez M, Trueba M, and Gomez-Munoz A**. Ceramide 1-phosphate (C1P) promotes cell migration Involvement of a specific C1P receptor. *Cell Signal* 21: 405-412, 2009.

24.	**Hamilton JA, Myers D, Jessup W, Cochrane F, Byrne R, Whitty G, and Moss S**. Oxidized LDL can induce macrophage survival, DNA synthesis, and enhanced proliferative response to CSF-1 and GM-CSF. *Arterioscler Thromb Vasc Biol* 19: 98-105, 1999.

25.	**Hammad SM, Pierce JS, Soodavar F, Smith KJ, Al Gadban MM, Rembiesa B, Klein RL, Hannun YA, Bielawski J, and Bielawska A**. Blood sphingolipidomics in healthy humans: impact of sample collection methodology. *J Lipid Res* 51: 3074-3087, 2010.

26.	**Hankins JL, Fox TE, Barth BM, Unrath KA, and Kester M**. Exogenous ceramide-1-phosphate reduces lipopolysaccharide (LPS)-mediated cytokine expression. *J Biol Chem* 286: 44357-44366, 2012.

27.	**Hundal RS, Salh BS, Schrader JW, Gomez-Munoz A, Duronio V, and Steinbrecher UP**. Oxidized low density lipoprotein inhibits macrophage apoptosis through activation of the PI 3-kinase/PKB pathway. *J Lipid Res* 42: 1483-1491, 2001.

28.	**Karapetyan AV, Klyachkin YM, Selim SM, Sunkara M, Ziada KM, Cohen DA, Zuba-Surma E, Ratajczak J, Smyth SS, Ratajczak MZ, Morris AJ, and Abdel-Latif A**. Bioactive Lipids and Cationic Antimicrobial Peptides As New Potential Regulators for Trafficking of Bone Marrow Derived Stem Cell In Patients With Acute Myocardial Infarction. *Stem Cells Dev* In press, 2013.

29.	**Kim C, Schneider G, Abdel-Latif A, Mierzejewska K, Sunkara M, Borkowska S, Ratajczak J, Morris AJ, Kucia M, and Ratajczak MZ**. Ceramide-1-phosphate Regulates Migration of Multipotent Stromal Cells (MSCs) and Endothelial Progenitor Cells (EPCs) - Implications for Tissue Regeneration. *Stem Cells* 31(3): 500-510, 2012.

30.	**Kim CH, Wu W, Wysoczynski M, Abdel-Latif A, Sunkara M, Morris A, Kucia M, Ratajczak J, and Ratajczak MZ**. Conditioning for hematopoietic transplantation activates the complement cascade and induces a proteolytic environment in bone marrow: a novel role for bioactive lipids and soluble C5b-C9 as homing factors. *Leukemia* 26: 106-116, 2011.

31.   **Kim K, Sohn H, Kim JS, Choi HG, Byun EH, Lee KI, Shin SJ, Song CH, Park JK, and Kim HJ**. Mycobacterium tuberculosis Rv0652 stimulates production of tumour necrosis factor and monocytes chemoattractant protein-1 in macrophages through the Toll-like receptor 4 pathway. *Immunology* 136: 231-240, 2012.

32.   **Lamour NF, Stahelin RV, Wijesinghe DS, Maceyka M, Wang E, Allegood JC, Merrill AH, Jr., Cho W, and Chalfant CE**. Ceramide kinase uses ceramide provided by ceramide transport protein: localization to organelles of eicosanoid synthesis. *J Lipid Res* 48: 1293-1304, 2007.

33.   **Lee DH, Kim SC, Joo JK, Kim HG, Na YJ, Kwak JY, and Lee KS**. Effects of 17beta-estradiol on the release of monocyte chemotactic protein-1 and MAPK activity in monocytes stimulated with peritoneal fluid from endometriosis patients. *J Obstet Gynaecol Res* 38: 516-525, 2012.

34.   **Lee HY, Lee SY, Kim SD, Shim JW, Kim HJ, Jung YS, Kwon JY, Baek SH, Chung J, and Bae YS**. Sphingosylphosphorylcholine stimulates CCL2 production from human umbilical vein endothelial cells. *J Immunol* 186: 4347-4353, 2011.

35.   **Li MQ, Li HP, Meng YH, Wang XQ, Zhu XY, Mei J, and Li DJ**. Chemokine CCL2 enhances survival and invasiveness of endometrial stromal cells in an autocrine manner by activating Akt and MAPK/Erk1/2 signal pathway. *Fertil Steril* 97: 919-929, 2012.

36.   **Lu X, and Kang Y**. Chemokine (C-C motif) ligand 2 engages CCR2+ stromal cells of monocytic origin to promote breast cancer metastasis to lung and bone. *J Biol Chem* 284: 29087-29096, 2009.

37.   **Martin P, and Leibovich SJ**. Inflammatory cells during wound repair: the good, the bad and the ugly. *Trends Cell Biol* 15: 599-607, 2005.

38.   **Martin P, and Parkhurst SM**. Parallels between tissue repair and embryo morphogenesis. *Development* 131: 3021-3034, 2004.

39.   **Mitsutake S, Date T, Yokota H, Sugiura M, Kohama T, and Igarashi Y**. Ceramide kinase deficiency improves diet-induced obesity and insulin resistance. *FEBS Lett* 586: 1300-1305, 2012.

40.   **Nixon GF, Mathieson FA, and Hunter I**. The multi-functional role of sphingosylphosphorylcholine. *Prog Lipid Res* 47: 62-75, 2008.

41.   **Oppenheim JJ, Zachariae CO, Mukaida N, and Matsushima K**. Properties of the novel proinflammatory supergene "intercrine" cytokine family. *Annu Rev Immunol* 9: 617-648, 1991.

42.   **Oskeritzian CA, Alvarez SE, Hait NC, Price MM, Milstien S, and Spiegel S**. Distinct roles of sphingosine kinases 1 and 2 in human mast-cell functions. *Blood* 111: 4193-4200, 2008.

43.   **Pettus BJ, Bielawska A, Subramanian P, Wijesinghe DS, Maceyka M, Leslie CC, Evans JH, Freiberg J, Roddy P, Hannun YA, and Chalfant CE**. Ceramide 1-phosphate is a direct activator of cytosolic phospholipase A2. *J Biol Chem* 279: 11320-11326, 2004.

44.   **Pettus BJ, Chalfant CE, and Hannun YA**. Sphingolipids in inflammation: roles and implications. *Curr Mol Med* 4: 405-418, 2004.

45.   **Pettus BJ, Kitatani K, Chalfant CE, Taha TA, Kawamori T, Bielawski J, Obeid LM, and Hannun YA**. The coordination of prostaglandin E2 production by sphingosine-1-phosphate and ceramide-1-phosphate. *Mol Pharmacol* 68: 330-335, 2005.

46.   **Pollard JW**. Tumour-educated macrophages promote tumour progression and metastasis. *Nat Rev Cancer* 4: 71-78, 2004.

47.   **Qian BZ, Li J, Zhang H, Kitamura T, Zhang J, Campion LR, Kaiser EA, Snyder LA, and Pollard JW**. CCL2 recruits inflammatory monocytes to facilitate breast-tumour metastasis. *Nature* 475: 222-225, 2011.

48.   **Ribeiro C, Petit V, and Affolter M**. Signaling systems, guided cell migration, and organogenesis: insights from genetic studies in Drosophila. *Dev Biol* 260: 1-8, 2003.

49.   **Rollins BJ**. Chemokines. *Blood* 90: 909-928, 1997.

50.   **Sanders SK, Crean SM, Boxer PA, Kellner D, LaRosa GJ, and Hunt SW, 3rd**. Functional differences between monocyte chemotactic protein-1 receptor A and monocyte chemotactic protein-1 receptor B expressed in a Jurkat T cell. *J Immunol* 165: 4877-4883, 2000.

51.   **Shimizu H, Bolati D, Higashiyama Y, Nishijima F, Shimizu K, and Niwa T**. Indoxyl sulfate upregulates renal expression of MCP-1 via production of ROS and activation of NF-kappaB, p53, ERK, and JNK in proximal tubular cells. *Life Sci* 90: 525-530, 2012.

52.   **Spiegel S, and Milstien S**. The outs and the ins of sphingosine-1-phosphate in immunity. *Nat Rev Immunol* 11: 403-415, 2011.

53.   **Takayama K, Garcia-Cardena G, Sukhova GK, Comander J, Gimbrone MA, Jr., and Libby P**. Prostaglandin E2 suppresses chemokine production in human macrophages through the EP4 receptor. *J Biol Chem* 277: 44147-44154, 2002.

54.   **Wirrig C, Hunter I, Mathieson FA, and Nixon GF**. Sphingosylphosphorylcholine is a proinflammatory mediator in cerebral arteries. *J Cereb Blood Flow Metab* 31: 212-221, 2011.

55.   **Yao HL, Gao FH, Li ZZ, Wu HX, Xu MD, Zhang Z, and Dai QY**. Monocyte chemoattractant protein-1 mediates angiotensin II-induced vascular smooth muscle cell proliferation via SAPK/JNK and ERK1/2. *Mol Cell Biochem* 366: 355-362, 2012.

56.   **Younce C, and Kolattukudy P**. MCP-1 Induced Protein Promotes Adipogenesis via Oxidative Stress, Endoplasmic Reticulum Stress and Autophagy. *Cell Physiol Biochem* 30: 307-320, 2012.

57.   **Zhang J, Patel L, and Pienta KJ**. CC chemokine ligand 2 (CCL2) promotes prostate cancer tumorigenesis and metastasis. *Cytokine Growth Factor Rev* 21: 41-48, 2010.

Figures legends

FIGURE 1. C1P induces MCP-1 release in J774A.1 macrophages. **A.** Cells were seeded in 24-well plates (2×10^4 cells/well) and incubated overnight in DMEM supplemented with 10% FBS. The cells were then washed and the medium was replaced by DMEM supplemented with 1% FBS. After 2 h of incubation, the macrophages were further incubated for 24 h with the indicated concentrations of C1P. MCP-1 concentration was measured by ELISA, as indicated in the *Materials and Methods* section. MCP-1 values were normalized to the total cell number and the results are expressed as the mean $\pm$ SEM of 5 independent experiments performed in duplicate. **B.** The cells were treated as in panel A, and incubated with 20 µM C1P for the indicated periods of time. MCP-1 concentration was determined as indicated in *Materials and Methods*. Values were normalized to the total cell number and the results are expressed as the mean $\pm$ SEM of 4 independent experiments performed in duplicate (*p<0.05; ***p<0.001).

FIGURE 2. The PI3K/Akt pathway is involved in C1P-stimulated MCP-1 release. Cells were seeded and treated as in figure 1. **A.** Cells were preincubated with 1 µM Ly 294002 (a selective PI3K inhibitor) (solid bars) or with vehicle (empty bars) for 30 min prior to stimulation with 20 µM C1P. The cells were then incubated further for 24 h and MCP-1 concentration was measured by ELISA, as indicated in the *Materials and Methods* section. MCP-1 values were normalized to the total cell number and the results are expressed as the mean $\pm$ SEM of 5 independent experiments performed in duplicate. **B.** Cells were preincubated with 1 µM 10-DEBC (a selective Akt inhibitor) (solid bars) or with vehicle (empty bars) for 30 min and then treated with 20 µM C1P for 24 h. MCP-1 concentration was determined by ELISA as indicated in the *Materials and Methods* section. The values were normalized to the total cell number and the results are expressed as the mean $\pm$ SEM of 5 independent experiments performed in duplicate. **C.** Cells were

seeded in 60 mm dishes (2 x 10^5 cells/dish) and treated with vehicle (empty bars),

negative siRNA (solid bars), or PI3K siRNA (hatched bars), as described in the *Materials

and Methods* section. Vehicle (control) or 20 µM C1P were then added for 24 h, as

indicated. Cells were then scraped and treated as in panel A. MCP-1 concentration was

determined by ELISA and normalized to the total cell number. **D.** Cells were incubated

and treated as in panel C except that siRNA Akt1 was used instead of PI3K siRNA. Data

are expressed as the mean ± SEM of 4 independent experiments performed in duplicate.

E. PI3K siRNA inhibitory efficiency was confirmed by Western blotting using specific

antibodies against PI3K. Equal loading of protein was monitored using a specific

antibody to GAPDH. Similar results were obtained in each of 2 independent experiments.

F. Results of scanning densitometry of the exposed film. Data are expressed as arbitrary

units of intensity and are the mean ± range of 2 independent experiments. **G.** Akt1 siRNA

inhibitory efficiency was confirmed by Western blotting using specific antibodies against

Akt1. Equal loading of protein was monitored using a specific antibody to GAPDH.

Similar results were obtained in each of 2 independent experiments. **H.** Results of

scanning densitometry of the exposed film. Data are expressed as arbitrary units of

intensity and are the mean ± range of 2 independent experiments. (n.s., no significant;

*p<0.05; **p<0.01).

FIGURE 3. The MEK/ERK pathway is involved in the stimulation of MCP-1 release by

C1P. **A.** Macrophages were seeded and treated as in figure 1, and were preincubated for

30 min with vehicle (empty bars) or with 10 µM PD 98059 to inhibit MEK (solid bars)

prior to stimulation with 20 µM C1P for 24 h, as indicated. MCP-1 concentration in the

medium was measured by ELISA (see *Materials and Methods* section) and the results are

the mean ± SEM of 6 independent experiments performed in duplicate. **B.** Cells were

seeded in 60 mm dishes (2 x 10^5 cells/dish) and treated with vehicle (empty bars),

negative siRNA (solid bars), or ERK siRNA (hatched bars), as described in the *Materials and Methods* section. The cells were then incubated with vehicle (Control) or with 20 µM C1P for 24 h, as indicated. MCP-1 concentration was normalized to the total cell number and data are expressed as the mean ± SEM of 5 independent experiments performed in duplicate. **C.** ERK siRNA inhibitory efficiency was confirmed by Western blotting using specific antibodies against ERK. Equal loading of protein was monitored using a specific antibody to GAPDH. Similar results were obtained in each of 2 independent experiments. **D.** Results of scanning densitometry of the exposed film. Data are expressed as arbitrary units of intensity and are the mean ± range of 2 independent experiments. (n.s., no significant; *p<0.05; **p<0.01).

FIGURE 4. p38 MAPK is implicated in C1P stimulated MCP-1 release. **A**. Macrophages were seeded and treated as in figure 1. The cells were preincubated with vehicle (empty bars) or with 1 µM SB 202190 (a selective inhibitor of p38) (solid bars) for 30 min prior to stimulation with 20 µM C1P for 24 h, as indicated. MCP-1 was measured by ELISA and normalized to the total cell number. Results are the mean ± SEM of 3 independent experiments performed in duplicate. **B.** Cells were seeded in 60 mm dishes (2 x 10^5 cells/dish) and treated with vehicle (empty bars), negative siRNA (solid bars), or p38α siRNA (hatched bars), as described in the *Materials and Methods* section. The cells were then incubated with vehicle (Control) or with 20 µM C1P for 24 h, as indicated. MCP-1 concentration was normalized and data are expressed as the mean ± SEM of 5 independent experiments performed in duplicate. **C.** p38α siRNA inhibitory efficiency was confirmed by Western blotting using specific antibodies against p38α. Equal loading of protein was monitored using a specific antibody to GAPDH. Similar results were obtained in each of 2 independent experiments. **D.** Results of scanning densitometry of

the exposed film. Data are expressed as arbitrary units of intensity and are the mean ± range of 2 independent experiments. (*p<0.05).

FIGURE 5. JNK is not implicated in C1P stimulated MCP-1 release. J774A.1 cells were seeded in 60 mm dishes (2 x 10^5 cells/dish) and siRNA treatment to silence JNK1 (panel A), JNK2 (panel B) and JNK3 (panel C) was performed as described in the Materials and Methods section. The cells were seeded and treated with vehicle (Control) or with 20 µM C1P for 24 h, as indicated. MCP-1 concentration was normalized and data are expressed as the mean ± SEM of 5 independent experiments performed in duplicate. siRNA inhibitory efficiency was confirmed by Western blotting using specific antibodies against JNK1(panel D), JNK2 (panel E) and JNK3 (panel F). Equal loading of protein was monitored using a specific antibody to GAPDH. Similar results were obtained in each of 2 independent experiments. Exposed films were scanned and data obtained by densitometry are expressed as arbitrary units of intensity (JNK1 panel G, JNK2 panel H and JNK3 panel I) and are the mean ± range of 2 independent experiments.

FIGURE 6. C1P induces phosphorylation of ERK1-2, p38 and Akt. Macrophages were seeded in 60 mm dishes (2.5 x 10^5 cells/dish) and treated as indicated in *Materials and Methods*. The cells were then treated with 20 µM C1P for various times, as indicated. **A.** Phosphorylated proteins were detected by Western blotting using specific antibodies against each phosphorylated kinase. Equal loading of protein was monitored using a specific antibody to total protein of each kinase. Similar results were obtained in each of 4 independent experiments. **B.** Results of scanning densitometry of the exposed film. Data are expressed as arbitrary units of intensity and are the mean ± SEM of 4 independent experiments (*p<0.05).

FIGURE 7. NF-κB is implicated in C1P-induced MCP-1 release. **A.** Macrophages were seeded in 60 mm dishes (2.5 x 10^5 cells/dish) and treated as in figure 6. The cells were stimulated with 20 µM C1P for various times, as indicated. Phosphorylation of the p65 subunit of NF-κB was detected by western blotting using a specific antibody to phospho-p65. Equal loading of protein was monitored using a specific antibody to β-actin. Similar results were obtained in each of 3 independent experiments **B.** Results of scanning densitometry of the exposed film. Data are expressed as arbitrary units of intensity and are the mean ± SEM of 3 independent experiments. **C.** J774A.1 cells were seeded and treated as in figure 1, and they were preincubated with vehicle (empty bars) or with the NF-κB inhibitor SC-514 (25 µM) (solid bars) for 30 min prior to stimulation with 20 µM C1P, as indicated. After 24 h, MCP-1 concentration was measured by ELISA, as described in *Materials and Methods* and normalized to total cell number. Results are the mean ± SEM of 5 independent experiments performed in duplicate (**p<0.01).

FIGURE 8. Stimulation of cell migration by MCP-1 and C1P. Macrophage migration was measured using the Boyden chamber-based cell migration assay, as described in the *Materials and Methods* section. Cells (5 x 10^4 cells/well) were plated in the upper wells of 24-well chambers coated with fibronectin, and incubated for 1h. **A.** Cells were stimulated with increasing concentrations of MCP-1 or with 20 µM C1P, as indicated, and incubated further for 24 h. Results are expressed relative to the control value and are the mean ± SEM of 6 independent experiments performed in duplicate. **B.** Cells were treated with 150 ng/ml of MCP-1 for the indicated time periods. Results are expressed relative to the value at 0 h and are the mean ± SEM of 5 independent experiments performed in duplicate **C.** The cells were stimulated with increasing concentrations of C1P, as indicated, and incubated further for 24 h. Results are expressed relative to time

at 0 h and are the mean ± SEM of 3 independent experiments performed in duplicate (*p<0.05; **p<0.01).

FIGURE 9. MCP-1 is essential for C1P-stimulated cell migration. **A.** Macrophages were seeded and treated as in figure 8, and they were incubated with the indicated concentrations of anti-MCP-1 antibody in the absence (squares) or presence (triangles) of 20 µM C1P. Results are the mean ± SEM of 4 independent experiments performed in duplicate. **B.** Cells were seeded in 60 mm dishes (2 x 10^5 cells/dish) and treated with vehicle (empty bars), negative siRNA (solid bars) or MCP-1 siRNA (hatched bars) as, indicated in the *Materials and Methods* section. Vehicle (Control) or 20 µM C1P were then added to the cells and they were incubated further for 24 h. Results are expressed relative to the control value and are the mean ± SEM of 4 independent experiments performed in duplicate. **C.** MCP-1 siRNA inhibitory efficiency was confirmed by Western blotting using specific antibodies against MCP-1. Equal loading of protein was monitored using a specific antibody to GAPDH. Similar results were obtained in each of 2 independent experiments. **D.** Results of scanning densitometry of the exposed film. Data are expressed as arbitrary units of intensity and are the mean ± range of 2 independent experiments. (*p<0.05; **p< 0.01).

FIGURE 10. The MCP-1 receptor (CCR2b) is involved in C1P-stimulated cell migration. **A.** Macrophage migration was measured as indicated in figure 8. The cells were preincubated for 1 h with vehicle (empty bars) or with 10 nM RS 102895 (a selective inhibitor of CCR2b) (solid bars), and then treated with 20 µM C1P or 150 ng/ml MCP-1 for 24 h, as indicated. Results are expressed relative to the control value and are the mean ± SEM of 4 independent experiments performed in duplicate. **B.** Cells were seeded in 60 mm dishes (2 x 10^5 cells/dish) and treated with vehicle (empty bars), negative siRNA (solid bars) or CCR2b siRNA (hatched bars), as described in the *Materials and Methods*

section. Vehicle (Control) or 20 µM C1P were then added to the cells, as indicated, and they were incubated further for 24 h. Results are expressed relative to the control values and are the mean ± SEM of 4 independent experiments performed in duplicate. **C.** CCR2b siRNA inhibitory efficiency was confirmed by Western blotting using specific antibodies against CCR2b. Equal loading of protein was monitored using a specific antibody to GAPDH. Similar results were obtained in each of 2 independent experiments. **D.** Results of scanning densitometry of the exposed film. Data are expressed as arbitrary units of intensity and are the mean ± range of 2 independent experiments. (*p<0.05; **p<0.01; #p<0.05 (cells treated with MCP-1 versus cells treated with MCP-1 and RS 102895).

FIGURE 11. Involvement of PI3K/Akt, MEK/ERK1-2, p38 and NF-κB in C1P-stimulated cell migration. **A.** Cells were seeded in 60 mm dishes (2 x 10^5 cells/dish) and treated with vehicle, negative siRNA or specific siRNA to inhibit ERK, PI3K, Akt, or p38α, as indicated (see *Materials and Methods)*. Vehicle (Control) or 20 µM C1P were then added to the cells and they were incubated further for 24 h. Results are expressed relative to the control value and are the mean ± SEM of 4 independent experiments performed in duplicate. **B.** Macrophages were seeded and treated as in figure 8. Cells were then preincubated with 10 µM PD 98059, 1 µM 10-DEBC, 1 µM SB 202190 or 25 µM SC-514 for 1 h. Then, the cells were treated with or without 20 µM C1P, as indicated, and incubated for 24 h. Results are the mean ± SEM of 4 independent experiments performed in duplicate (n.s. no significant; *p<0.05).

FIGURE 12. Inhibition of C1P-stimulated MCP-1 release and macrophage migration by pertussis toxin **A**. Cells were seeded and treated as in figure 1. Macrophages were preincubated for 16 h with vehicle (empty bars) or with 10 pg/ml Ptx (solid bars). Then, vehicle (Control) or 20 µM C1P were added and cells were further incubated for 24 h. The medium was collected and MCP-1 concentration was determined by ELISA as

indicated in the *Materials and Methods* section. MCP-1 values were normalized to the total cell number and the results are expressed as the mean ± SEM of 4 independent experiments performed in duplicate. **B.** Macrophage migration was measured as in figure 8 (see *Materials and Methods*). The cells were preincubated for 4 h in the absence (empty bars) or presence (solid bars) of 10 pg/ml Ptx, and then treated with vehicle (Control) or with 20 µM C1P, as indicated, for 24 h. Results are the mean ± SEM of 4 independent experiments performed in duplicate (*p<0.05; **p<0.01).

FIGURE 13. The stimulation of MCP-1 release and cell migration by C1P are independent of interaction with sphingosine 1-phosphate receptors. Cells were seeded in 60 mm dishes (2×10^5 cells/dish) and treated with vehicle, negative siRNA, or with S1PR1 siRNA, S1PR2 siRNA, S1PR3, S1PR4 or S1PR5 siRNA as indicated. **A.** The cells were then seeded as in figure 1 and treated with vehicle (Control) or with 20 µM C1P for 24 h, as indicated. MCP-1 concentration was normalized and data are expressed as the mean ± SEM of 5 independent experiments performed in duplicate. **B.** Macrophage migration was measured as in figure 8 (see *Materials and Methods*). The cells were treated with vehicle (Control) or with 20 µM C1P, as indicated, for 24 h. Results are the mean ± SEM of 5 independent experiments performed in duplicate. **C.** S1PR1 siRNA inhibitory efficiency was confirmed by Western blotting using specific antibodies against S1PR1. Equal loading of protein was monitored using a specific antibody to GAPDH. Similar results were obtained in each of 2 independent experiments. **D.** Results of scanning densitometry of the exposed film. Data are expressed as arbitrary units of intensity and are the mean ± range of 2 independent experiments. **E.** S1PR2 siRNA inhibitory efficiency was confirmed by Western blotting using specific antibodies against S1PR2. Equal loading of protein was monitored using a specific antibody to GAPDH. Similar results were obtained in each of 2 independent experiments. **F.** Results of

scanning densitometry of the exposed film. Data are expressed as arbitrary units of intensity and are the mean ± range of 2 independent experiments. **G.** S1PR3 siRNA inhibitory efficiency was confirmed by Western blotting using specific antibodies against S1PR3. Equal loading of protein was monitored using a specific antibody to GAPDH. Similar results were obtained in each of 2 independent experiments. **H.** Results of scanning densitometry of the exposed film. Data are expressed as arbitrary units of intensity and are the mean ± range of 2 independent experiments. **I.** S1PR4 siRNA inhibitory efficiency was confirmed by Western blotting using specific antibodies against S1PR4. Equal loading of protein was monitored using a specific antibody to GAPDH. Similar results were obtained in each of 2 independent experiments. **J.** Results of scanning densitometry of the exposed film. Data are expressed as arbitrary units of intensity and are the mean ± range of 2 independent experiments. **K.** S1PR5 siRNA inhibitory efficiency was confirmed by Western blotting using specific antibodies against S1PR5. Equal loading of protein was monitored using a specific antibody to GAPDH. Similar results were obtained in each of 2 independent experiments. **L.** Results of scanning densitometry of the exposed film. Data are expressed as arbitrary units of intensity and are the mean ± range of 2 independent experiments.

FIGURE 14. C1P stimulates MCP-1 release and cell migration in human THP-1 monocytes. **A.** Cells were seeded in 24-well plates (10^5 cells/well) in RPMI as described in the *Materials and Methods section*. After 2 h, monocytes were incubated for 24 h with the indicated concentrations of C1P. MCP-1 concentration was measured by ELISA, as indicated in the *Materials and Methods* section. MCP-1 values were normalized to the total cell number and the results are expressed as the mean ± SEM of 4 independent experiments performed in duplicate. **B.** Macrophage migration was measured using the Boyden chamber-based cell migration assay, as described in the *Materials and Methods*

section. Cells (10^5 cells/well) were plated in the upper wells of 24-well chambers coated with fibronectin, and incubated for 1h. The cells were then stimulated with the indicated concentrations of C1P and incubated further for 24 h. Results are expressed relative to the control value and are the mean ± SEM of 4 independent experiments performed in duplicate. **C.** Cells were seeded as in panel B, and they were incubated without (empty bars) or with 0.5 µg/ml of anti-MCP-1 antibody (solid bars) in the absence or presence of 20 µM C1P, as indicated. Results are the mean ± SEM of 4 independent experiments performed in duplicate (*p<0.05; **p<0.01).

FIGURE 15. C1P stimulates MCP-1 release and cell migration in 3T3-L1 pre-adipocytes. **A.** Cells were seeded in 24-well plates (10^4 cells/well) in DMEM supplemented with 10% FCS, overnight. Then, the medium was replaced by DMEM without FCS and further incubated for 2 h. The cells were then incubated for 24 h with the indicated concentrations of C1P. MCP-1 concentration was measured by ELISA, as indicated in the *Materials and Methods* section. MCP-1 values were normalized to the total cell number and the results are expressed as the mean ± SEM of 4 independent experiments performed in duplicate. **B.** 3T3-L1 migration was measured using the Boyden chamber-based cell migration assay, as described in the *Materials and Methods* section. Cells (5 x 10^4 cells/well) were plated in the upper wells of 24-well chambers coated with fibronectin, and incubated for 1h. Cells were stimulated with indicated concentrations of C1P and incubated further for 24 h. Results are expressed relative to the control value and are the mean ± SEM of 4 independent experiments performed in duplicate. **C.** Cells were seeded as in panel B, and they were incubated without (empty bars) or with 0.5 µg/ml of anti-MCP-1 antibody (solid bars) in the absence or presence of 20 µM C1P, as indicated. Results are the mean ± SEM of 4 independent experiments performed in duplicate (*p<0.05; **p<0.01).
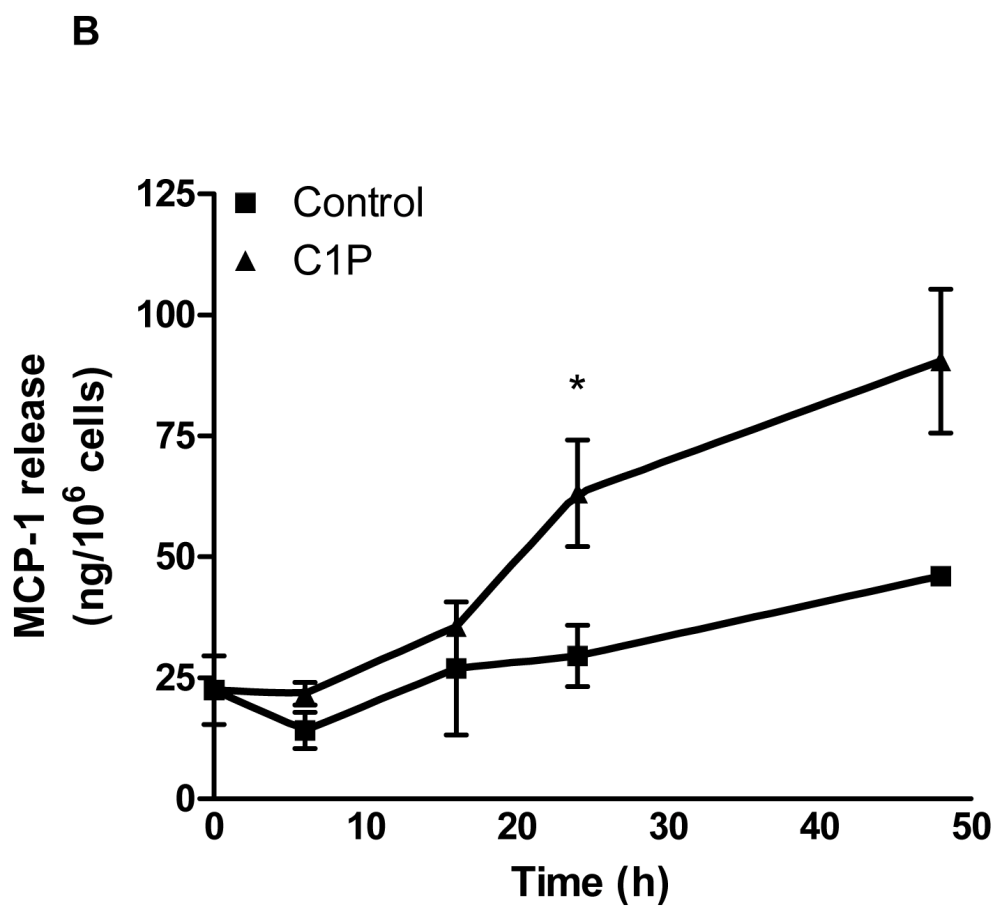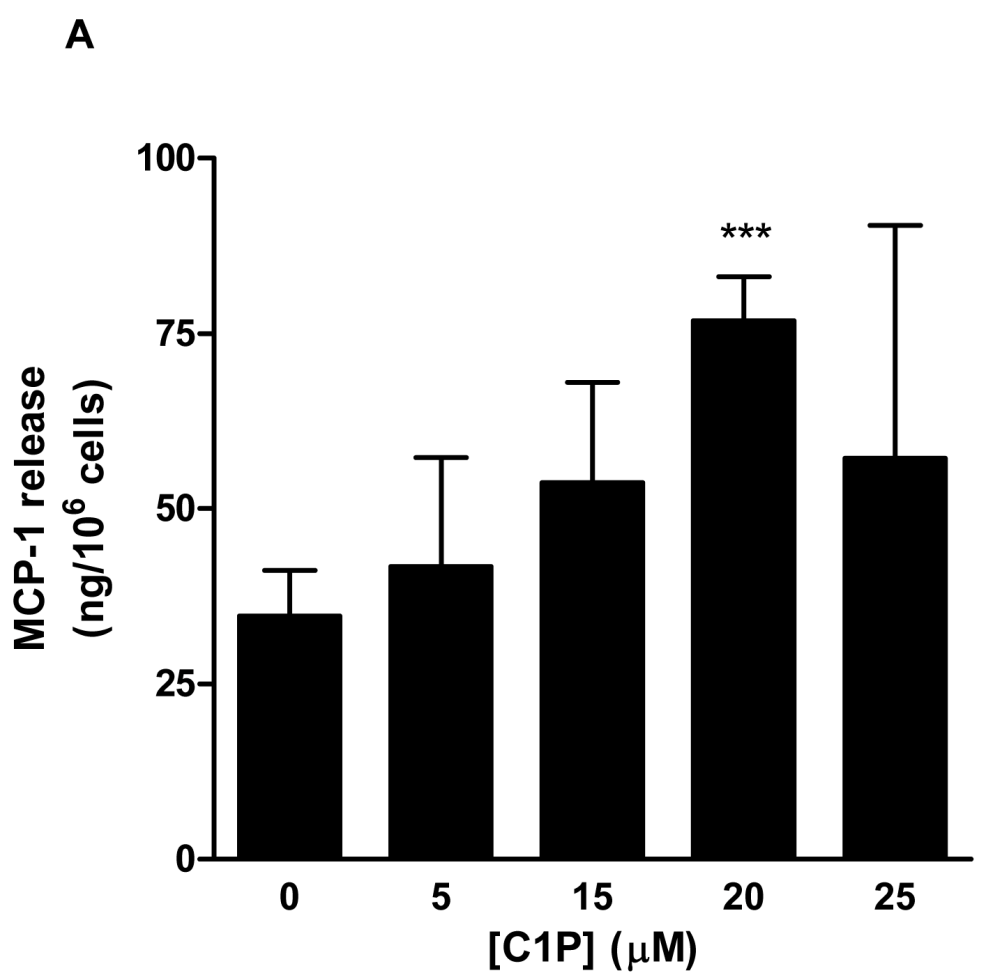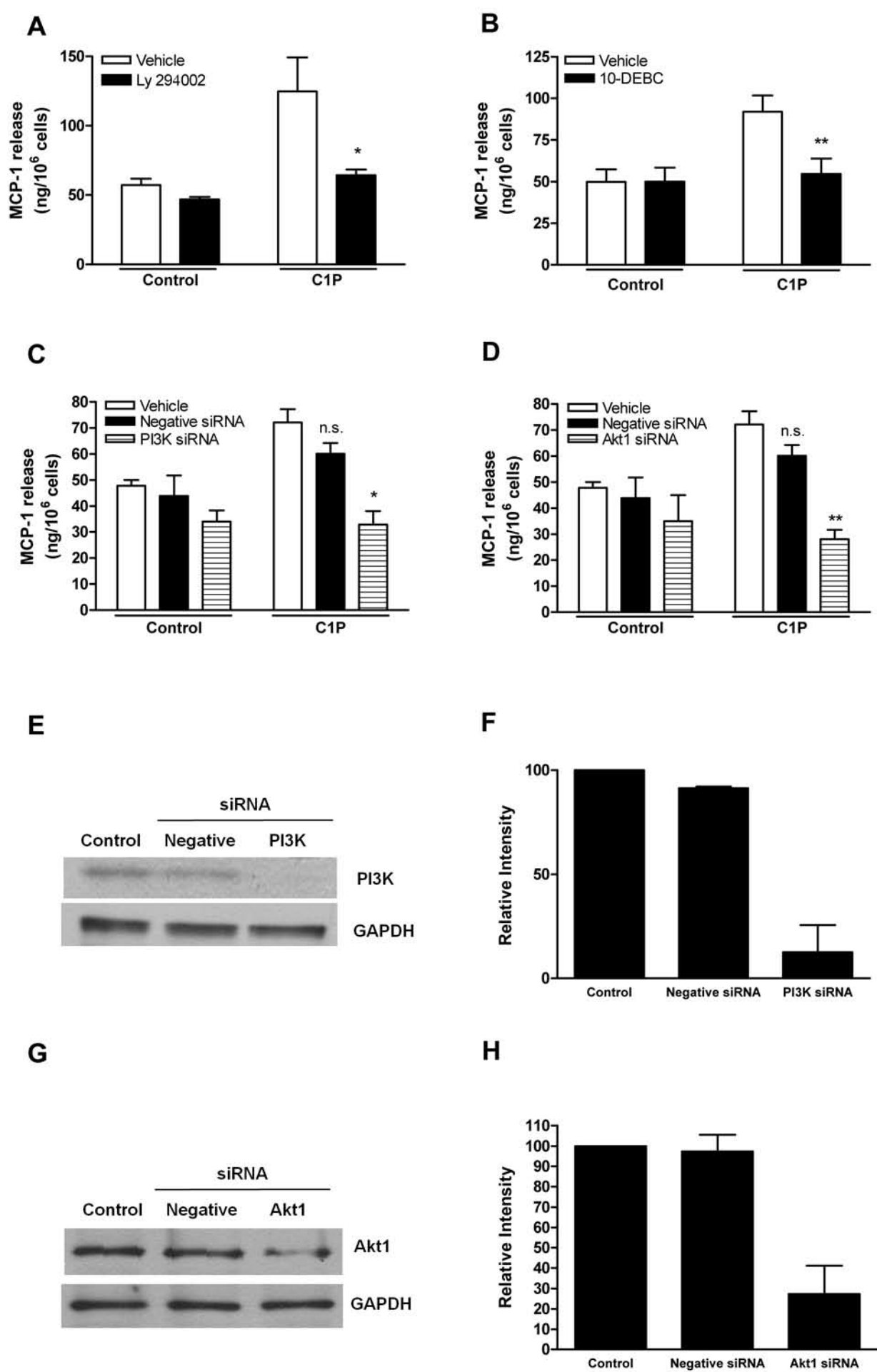
Figure 1

Figure 2
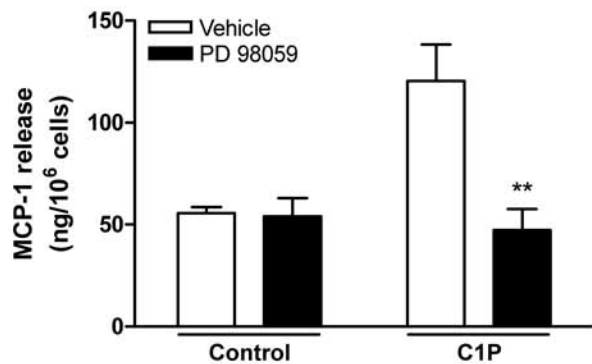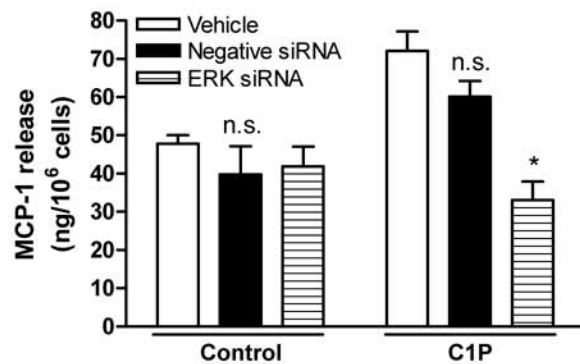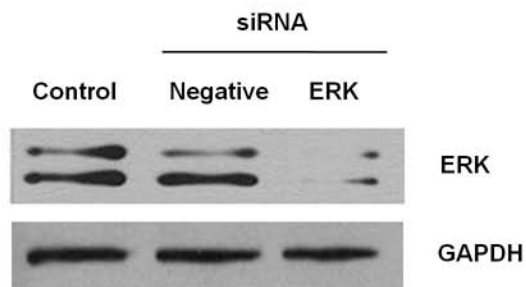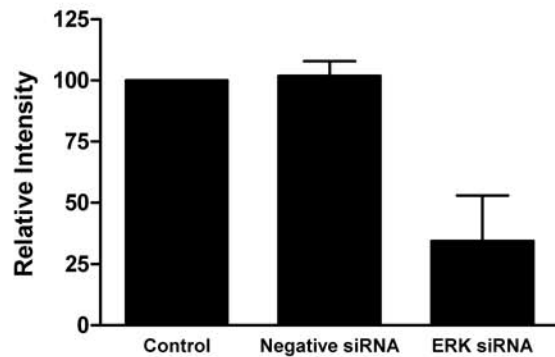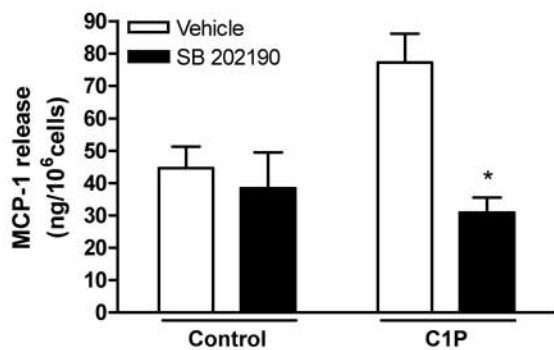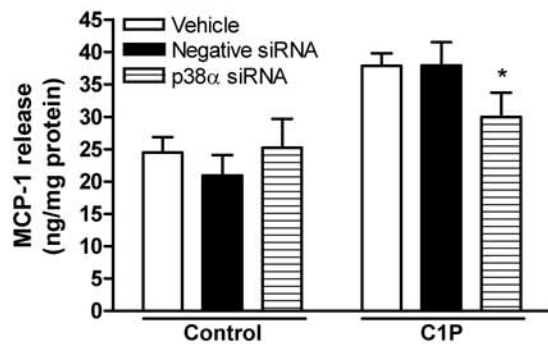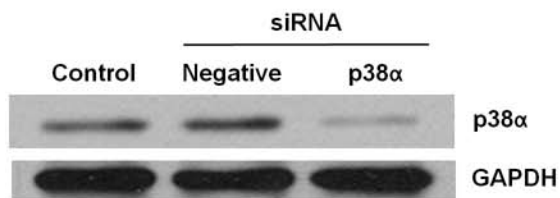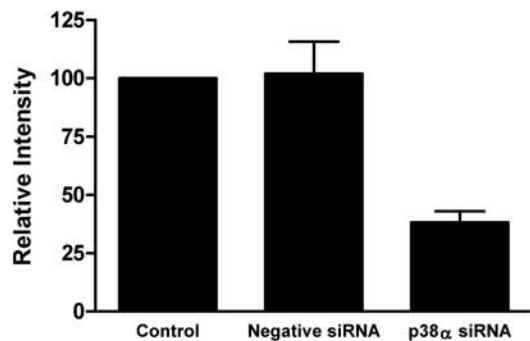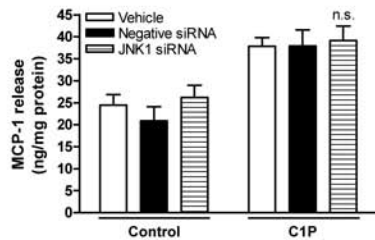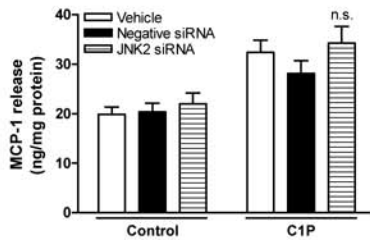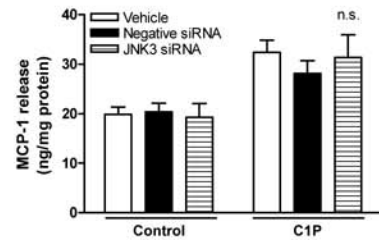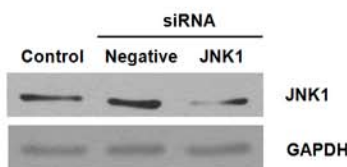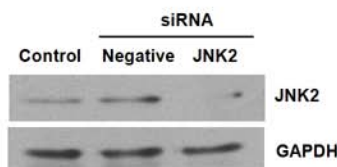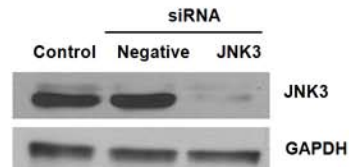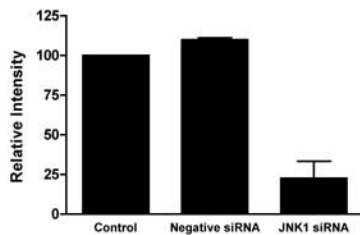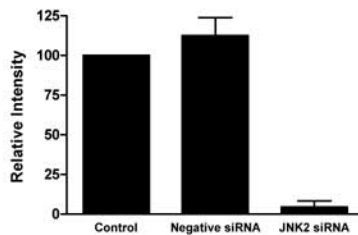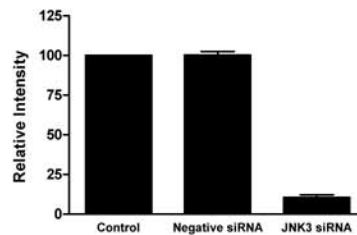
Figure 3
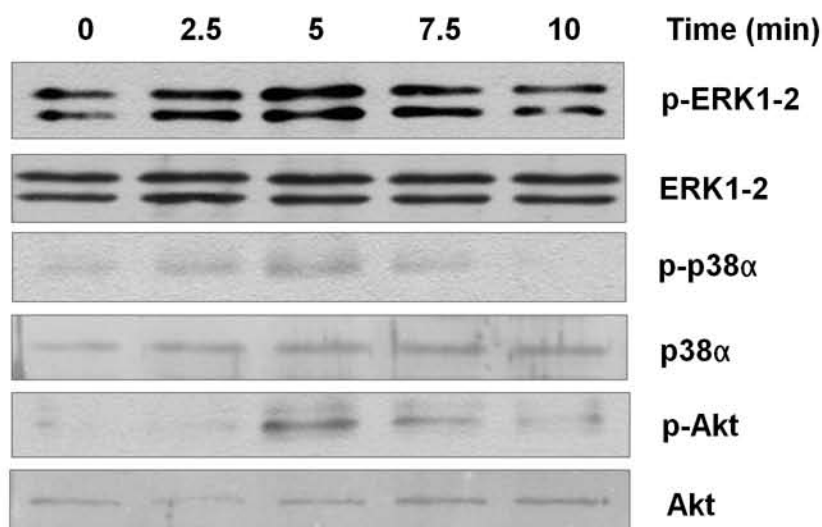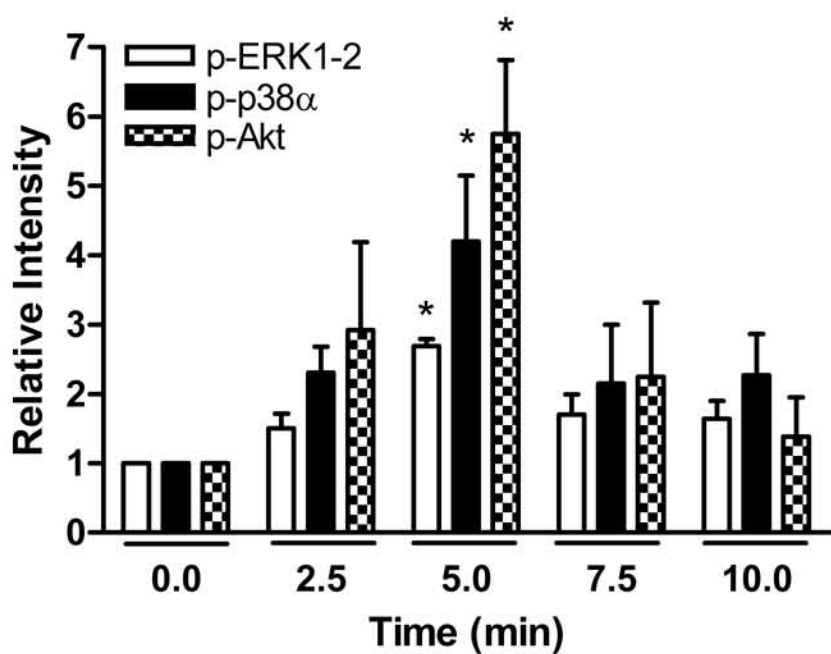
Figure 4

Figure 5

Figure 6

A

B

C
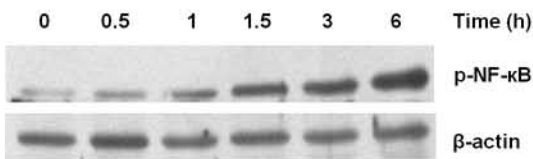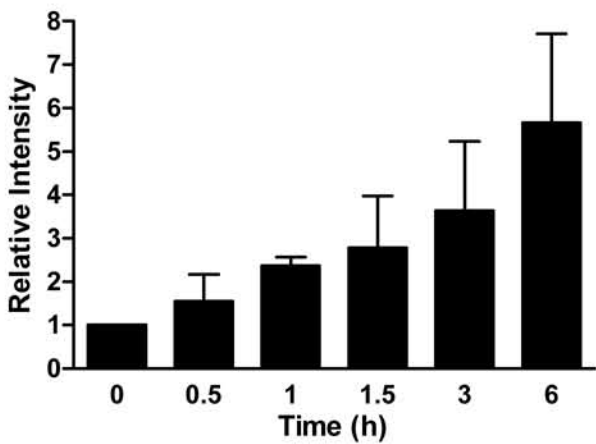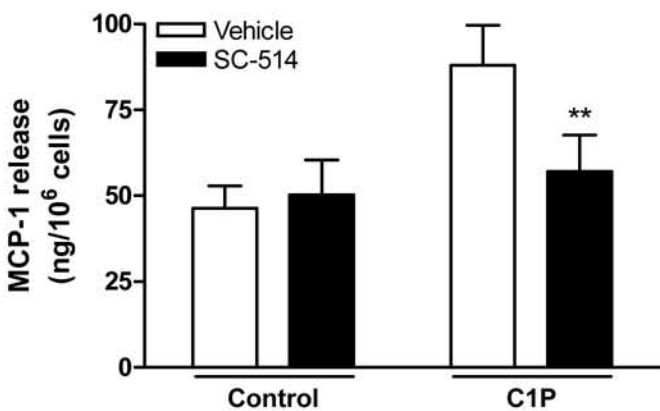
Figure 7
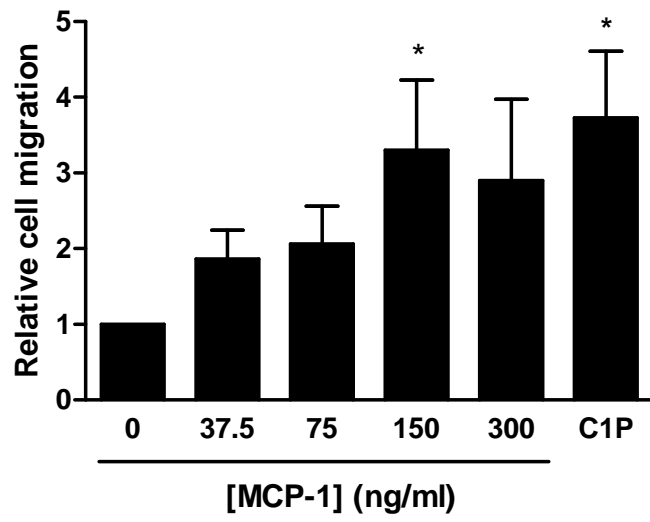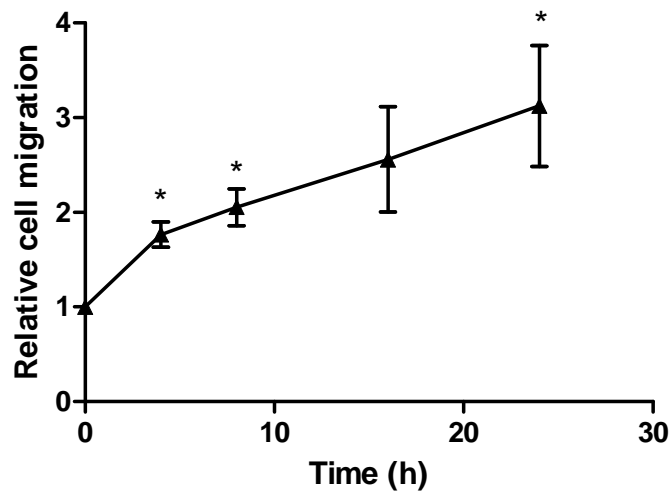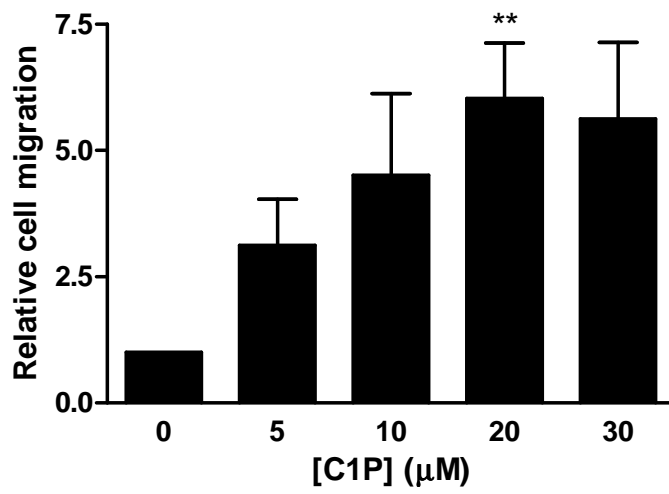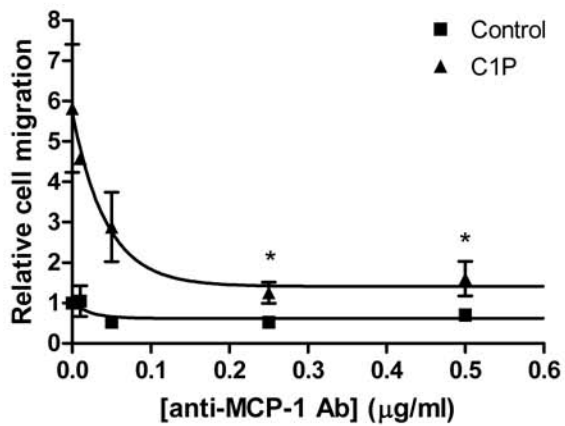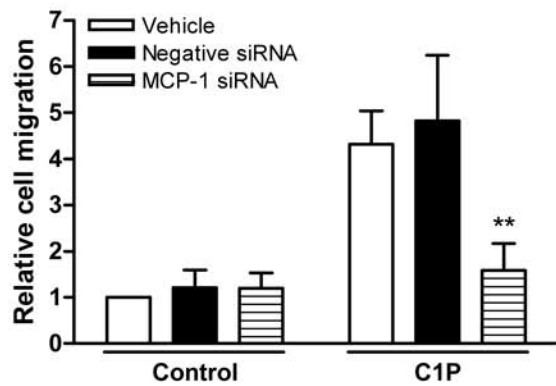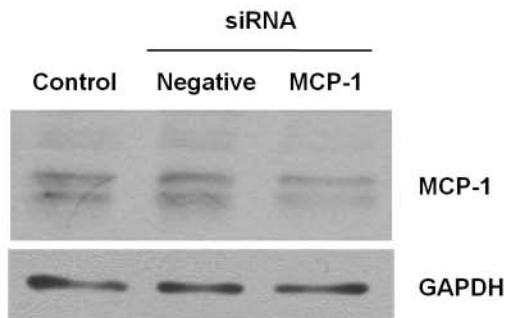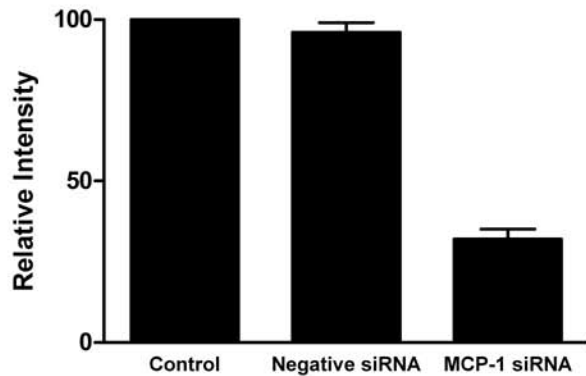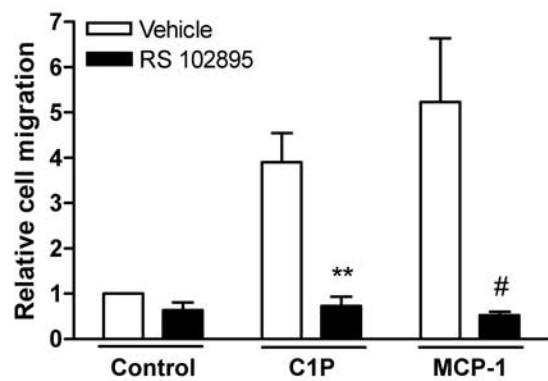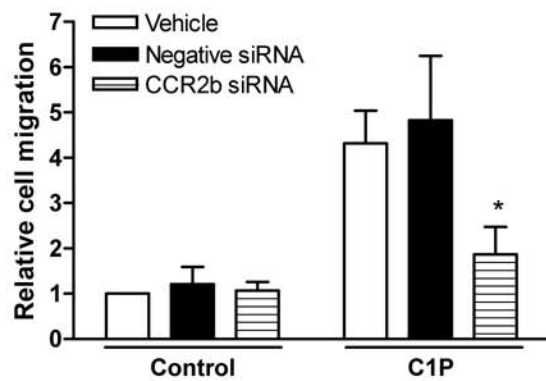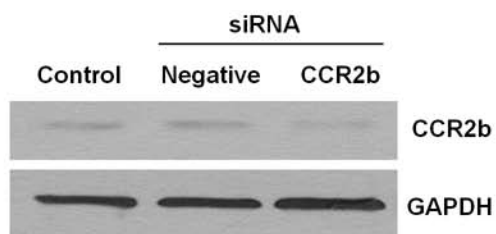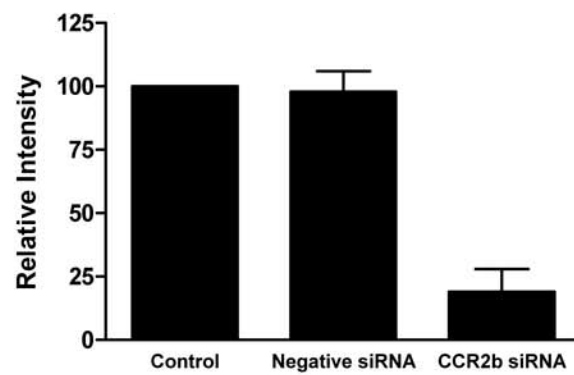
Figure 8

Figure 9

Figure 10

A
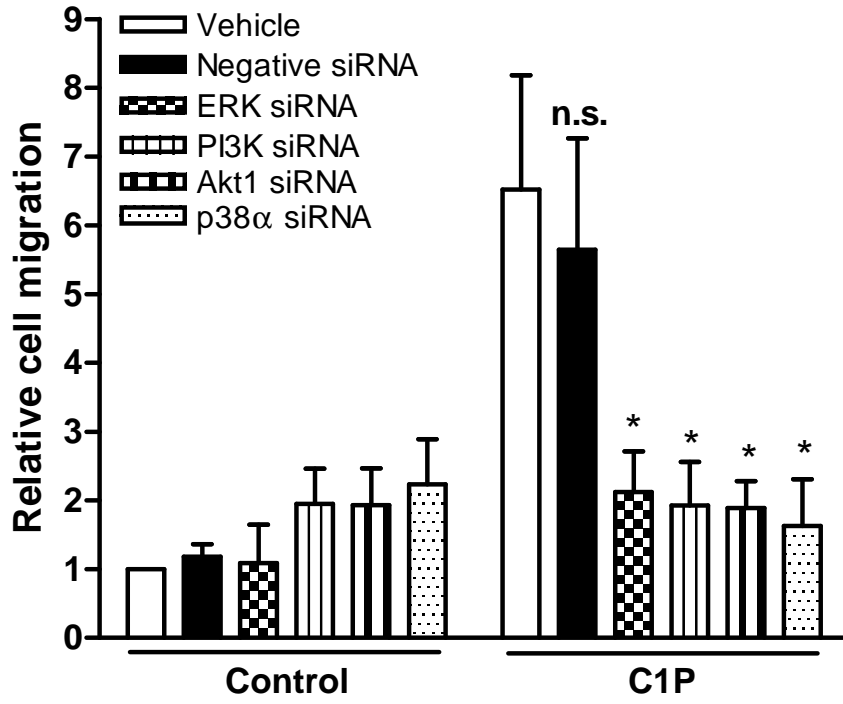
B
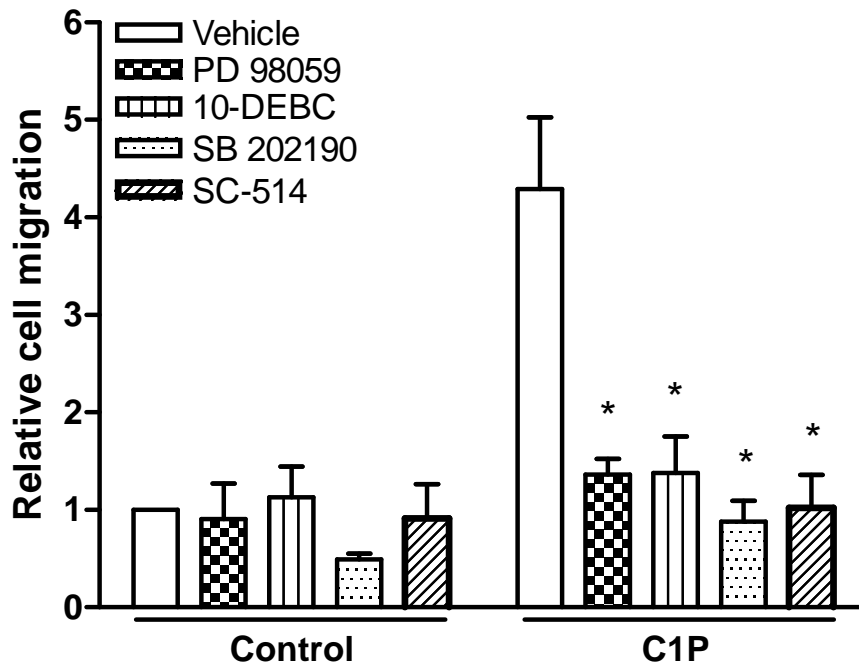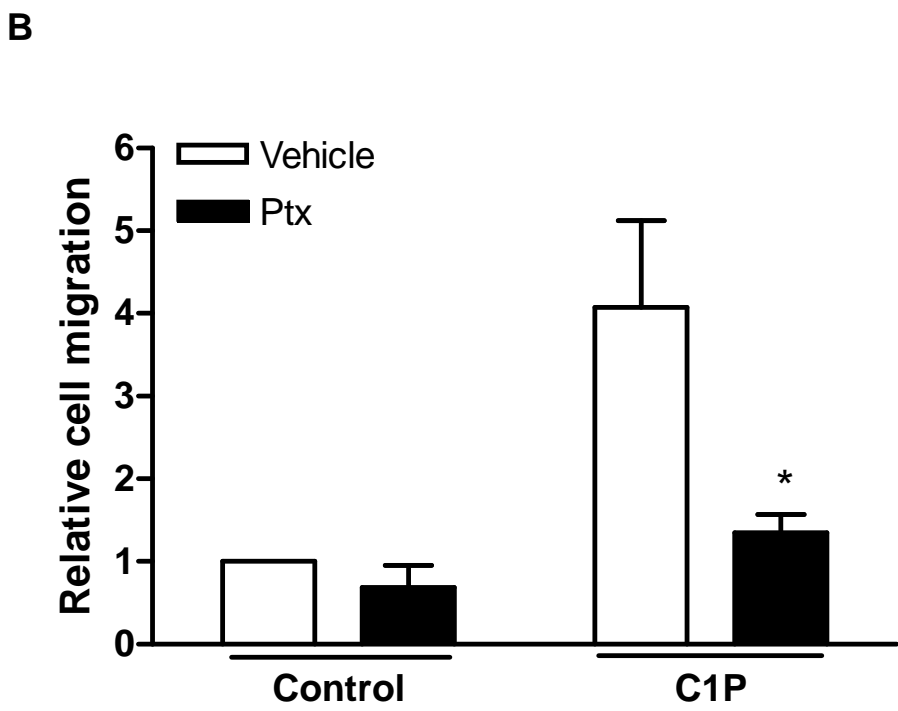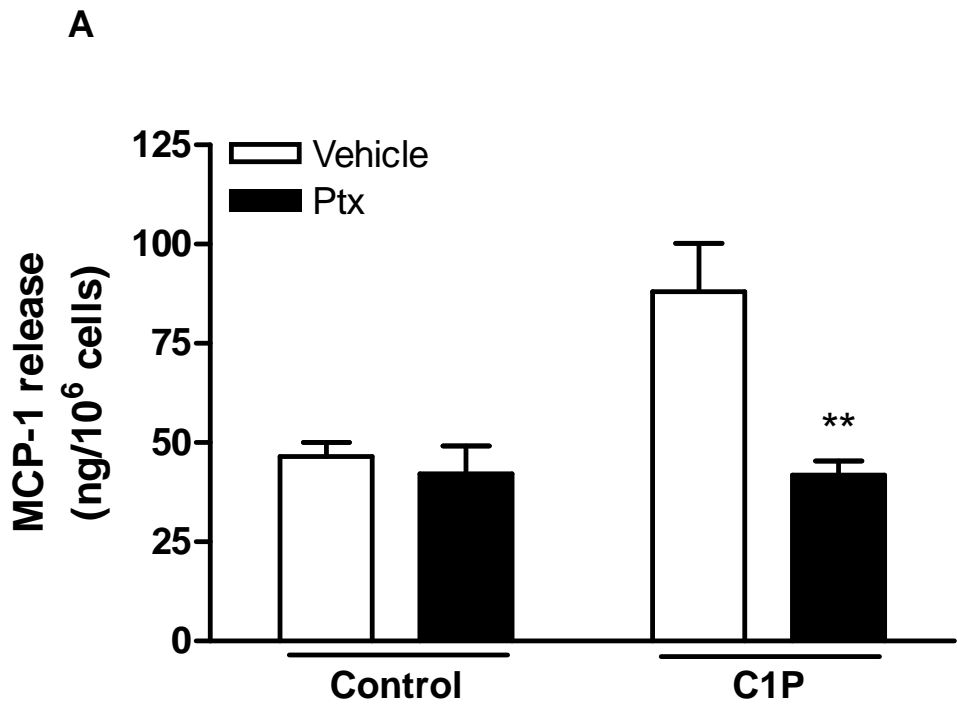
Figure 11

Figure 12
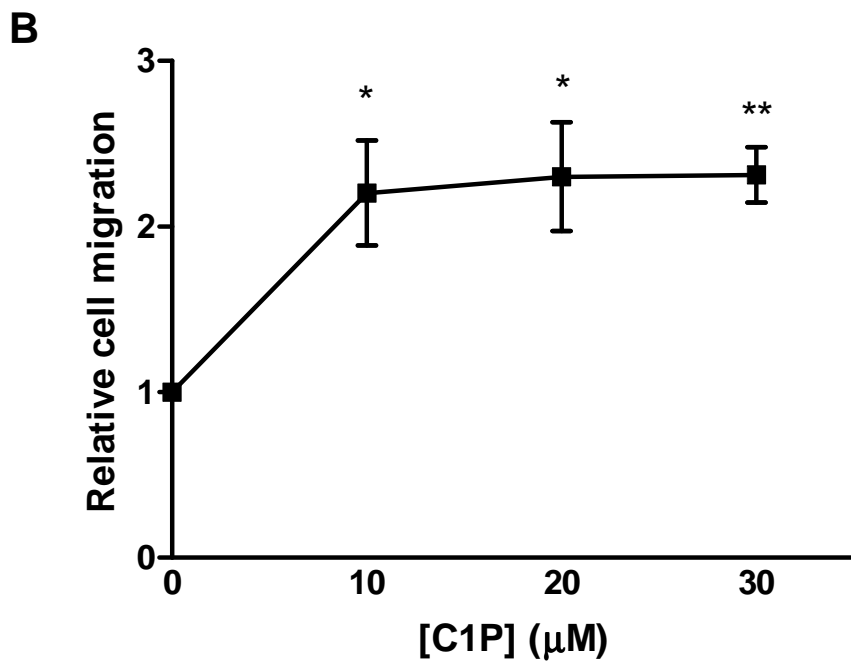
Figure 13
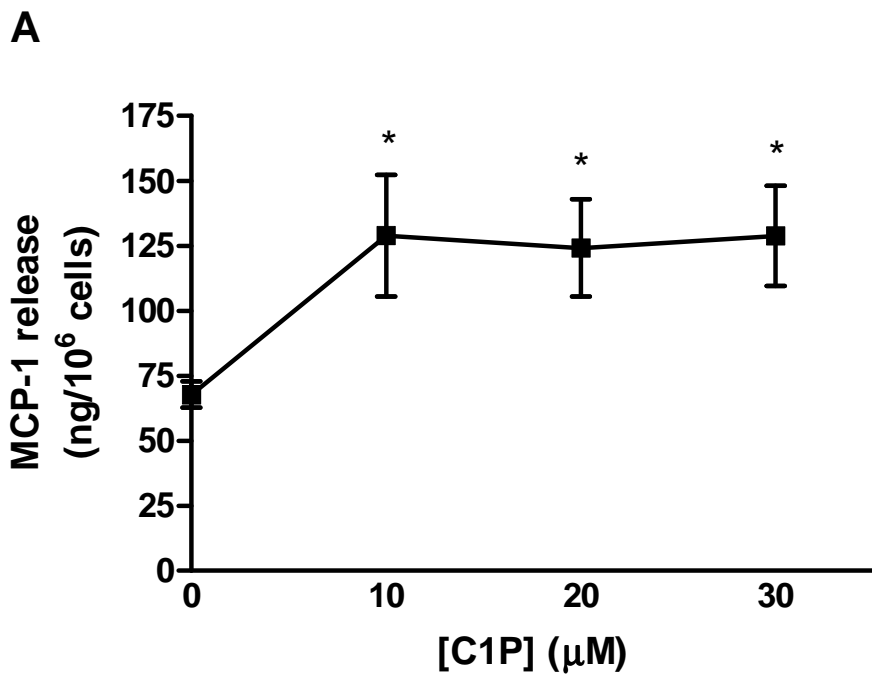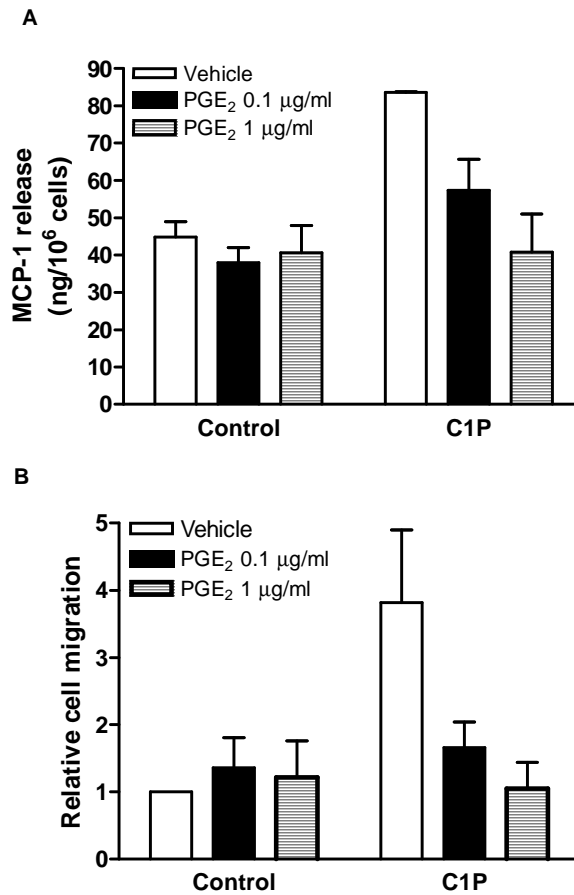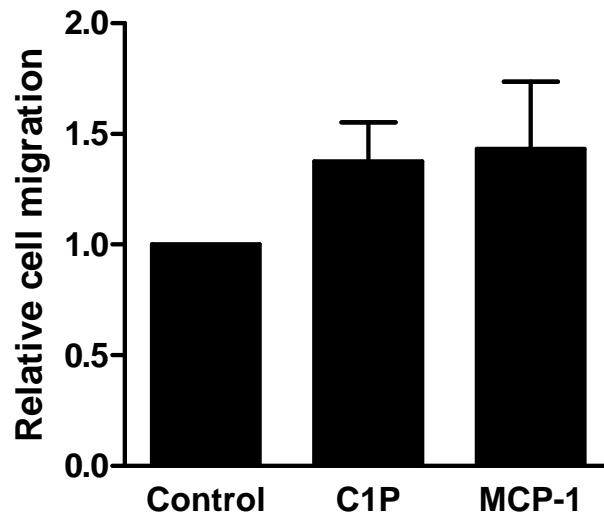
Figure 14

A

B

C
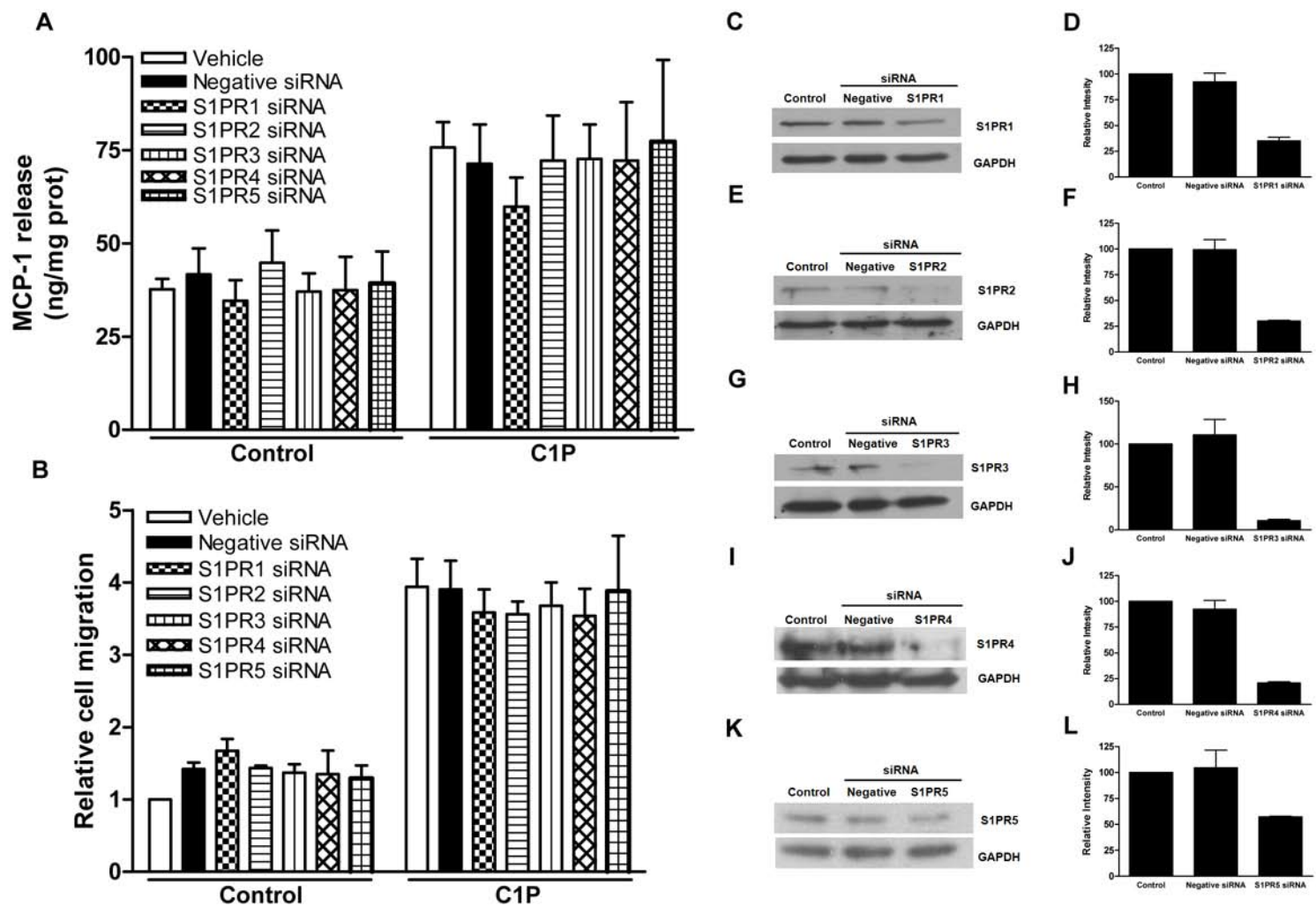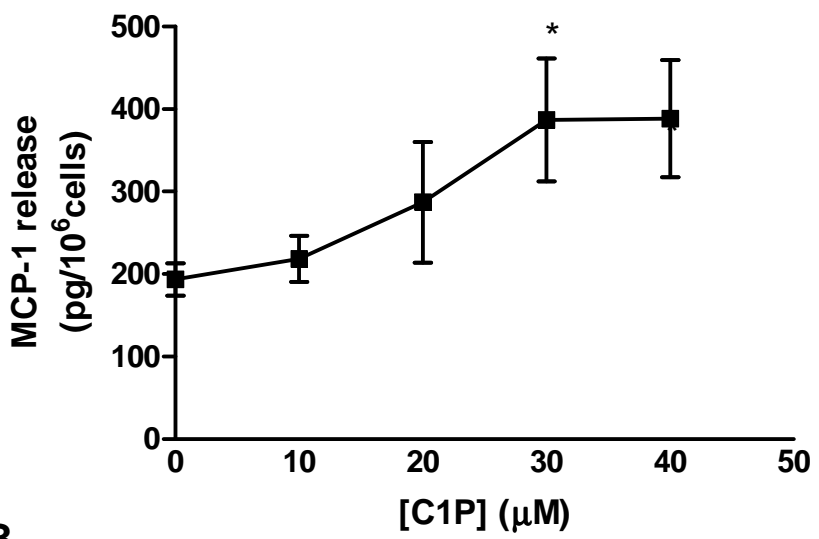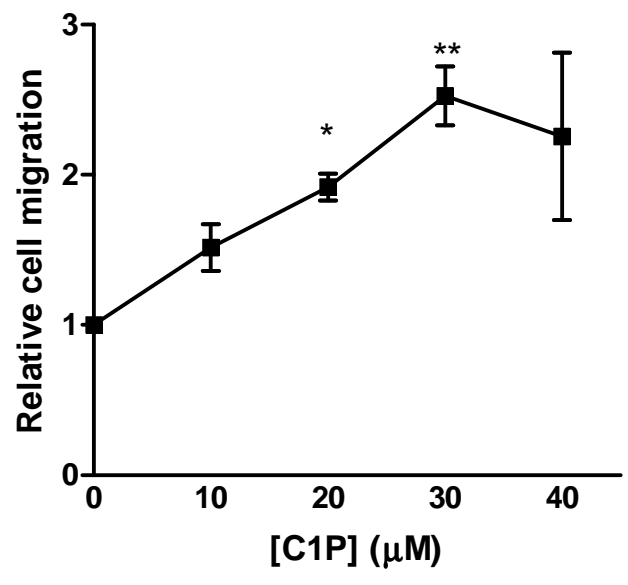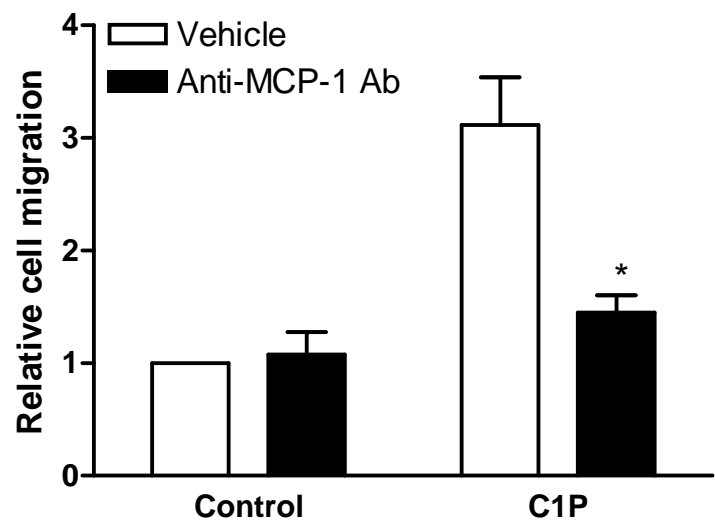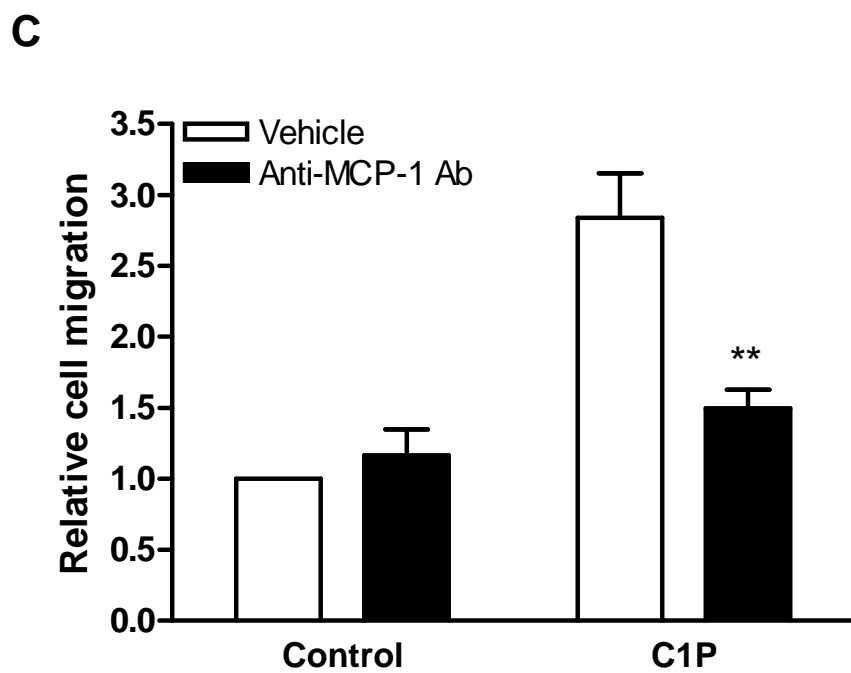
Figure 15

SUPPLEMENTARY FIGURE 1. Inhibition of C1P-stimulated MCP-1 release and macrophage migration by prostaglandin E_2 (PGE$_2$). **A.** Macrophages were seeded and treated as in figure 1. Cells were treated with the indicated concentrations of PGE$_2$ with or without 20 µM C1P, as indicated. The cells were then incubated for 24 h. The medium was collected and MCP-1 concentration was determined by ELISA as indicated in the *Materials and Methods* section. MCP-1 values were normalized to the total cell number and the results are expressed as the mean ± SEM of 3 independent experiments performed in duplicate. **B.** Macrophage migration was measured as in figure 8 (see *Materials and Methods*). The cells were treated with the indicated concentrations of PGE$_2$ with or without 20 µM C1P, for 24 h. Results are the mean ± range of 2 independent experiments performed in duplicate.

SUPPLEMENTARY FIGURE 2. Stimulation of cell migration by C1P and MCP-1 in bone marrow-derived macrophages (BMDM)**.** Macrophages were seeded as described in *Materials and Methods* section. Cell migration was measured using the Boyden chamber-based cell migration assay (see *Materials and Methods* section). Cells (1.5 x 10^5 cells/well) were plated in the upper wells of 24-well chambers coated with fibronectin, and incubated for 1h. The cells were then stimulated with vehicle, 20 µM C1P or 150 ng/ml MCP-1 and incubated further for 24 h. Results are expressed relative to the control value and are the mean ± range of 2 independent experiments performed in duplicate.